To the Graduate Council:

I am submitting herewith a thesis written by Ching Chuen Chan entitled "An Analysis of Improved Gaseous Insulating Mixtures in Practical Systems." I recommend that it be accepted in partial fulfillment of the requirements for the degree of Master of Science, with a major in Electrical Engineering.

Marshall O. Pace

Marshall O. Pace, Major Professor

We have read this thesis
and recommend its acceptance:

Igor Alexeff

L. G. Christophorou

Accepted for the Council:

L Evans Hall

Vice Chancellor
Graduate Studies and Research

AN ANALYSIS OF IMPROVED GASEOUS INSULATING MIXTURES IN PRACTICAL SYSTEMS

A Thesis

Presented for the

Master of Science

Degree

The University of Tennessee, Knoxville

Ching Chuen Chan

March 1979

1091444

ACKNOWLEDGEMENT

The author is grateful for the guidance and assistance of his advisor, Dr. Marshall O. Pace, with whom he works for the U. S. Department of Energy through Contract No. w-7405-eng-26 with Union Carbide Corporation, Nuclear Division. Appreciation is also expressed to Dr. I. Alexeff and Dr. L. G. Christophorou for the valuable suggestions they have made to clarify and to improve this thesis. It is also the author's desire to acknowledge his colleaques at Oak Ridge National Laboratory for their cooperation and inspiration. Special thanks to R. A. Mathis who has helped to set up the experimental apparatus and instrumentation.

Recognition is given to Miss Miranda Choi for typing up this thesis.

ABSTRACT

As transmission line voltages continue to go up, the need of better gaseous insulators has become more and more imminent. This research investigates the dielectric strengths of some improved gaseous insulating mixtures in small scale simulations of practical systems. Concentric cylinder geometries are used in this research to simulate underground transmission pipe lines. Knowledge of fundamental low-energy (mostly $\lesssim$ 10eV) electron-molecule interactions is being applied to the design of new improved gaseous dielectrics. It has been found that the electron attachment and slowing-down properties of dielectric gases/mixtures as a function of electron energy are very significant in designing gaseous insulators. Several binary gaseous systems (2-C_4F_6/N_2, c-C_4F_8/N_2, 2-C_4F_8/N_2) have been tested and found to be superior to the breakdown strengths of SF_6 mixtures. The properties of these practical systems such as the effects of surface roughness of electrodes, particle contaminants and electrode materials are also investigated.

TABLE OF CONTENTS

CHAPTER		PAGE
I.	INTRODUCTION	1
II.	THEORETICAL ANALYSIS	3
	Electrical Breakdown Mechanisms of Gases	4
	The Townsend Theory	5
	The Streamer Theory	7
	Prevention of Breakdown of Gases by Electron-Molecule Interactions	10
	Electron Attachment of Dielectric Gases/ Mixtures as Functions of Electron Energy	12
	Electron Slowing-down Properties of Dielectric Gases/Mixtures as Functions of Electron Energy	14
III.	EXPERIMENTAL ANALYSIS	16
	Experimental Apparatus	19
	Chamber	19
	Electrodes	20
	Electrical System of Apparatus	24
	Experimental Procedure and Techniques	26
	Breakdown Results	28
	The Breakdown of Gases/Mixtures Between Smooth Electrodes	29
	The Effects of Surface Roughness	35
	The Effects of Electrode Materials	49
	The Effects of Particle Contaminants	52
IV.	CONCLUSION	56

CHAPTER PAGE

LIST OF REFERENCES 61

APPENDIX 64

VITA 66

LIST OF FIGURES

FIGURE		PAGE
1.	Electron Attachment Cross Section Versus Electron Energy for 2-C_4F_6, c-C_4F_8, 2-C_4F_8, and SF_6	13
2.	Vibrational Excitation Cross Sections Versus Electron Energy for N_2	15
3.	Interior of Shielding Cage of Cylindrical Electrode Facility	17
4.	Exterior View of the Shielding Cage of Cylindrical Electrode Facility	18
5.	Outer Electrode Assembly for Concentric Cylinder Electrode Geometry	21
6.	Mounted Concentric Cylinder Electrodes	22
7.	Inner Electrodes for Concentric Cylinder Geometry .	23
8.	Breakdown Voltages for SF_6/N_2 Mixtures with Smooth Inner Electrodes	30
9.	Breakdown Voltages for c-C_4F_8/N_2 Mixtures with Smooth Inner Electrodes	31
10.	Breakdown Voltages for 2-C_4F_8/N_2 Mixtures with Smooth Inner Electrodes	32
11.	Breakdown Voltages for 2-C_4F_6/N_2 Mixtures with Smooth Inner Electrodes	33
12.	Breakdown Voltages for SF_6/N_2 and Fluorocarbon/N_2 Mixtures with 0.75-cm Radius Inner Electrode and 0.004-in. Groove Depth at Positive Potential	36
13.	Breakdown Voltages for SF_6/N_2 and Fluorocarbon/N_2 Mixtures with 0.75-cm Radius Inner Electrode and 0.004-in. Groove Depth at Negative Potential	37
14.	Breakdown Voltages for SF_6/N_2 and Fluorocarbon/N_2 Mixtures with 0.75-cm Radius Inner Electrode and 0.020-in. Groove Depth at Positive Potential	38
15.	Breakdown Voltages for SF_6/N_2 and Fluorocarbon/N_2 Mixtures with 0.75-cm Radius Inner Electrode and 0.020-in. Groove Depth at Negative Potential	39

FIGURE PAGE

16. Ratios of Breakdown Voltages for SF_6/N_2 Mixtures with Rough (grooved) Inner Electrodes (V_R) and with Smooth Electrodes (V_{SM}) of 0.75-cm Radius at Positive Potential 41

17. Ratios of Breakdown Voltages for SF_6/N_2 Mixtures with Rough (grooved) Inner Electrodes (V_R) and with Smooth Electrodes (V_{SM}) of 0.75-cm Radius at Negative Potential 42

18. Ratios of Breakdown Voltages for c-C_4F_8/N_2 Mixtures with Rough (grooved) Inner Electrodes (V_R) and with Smooth Electrodes (V_{SM}) of 0.75-cm Radius at Positive Potential 43

19. Ratios of Breakdown Voltages for c-C_4F_8/N_2 Mixtures with Rough (grooved) Inner Electrodes (V_R) and with Smooth Electrodes (V_{SM}) of 0.75-cm Radius at Negative Potential 44

20 Ratios of Breakdown Voltages for 2-C_4F_8/N_2 Mixtures with Rough (grooved) Inner Electrodes (V_R) and with Smooth Electrodes (V_{SM}) of 0.75-cm Radius at Positive Potential 45

21. Ratios of Breakdown Voltages for 2-C_4F_8/N_2 Mixtures with Rough (grooved) Inner Electrodes (V_R) and with Smooth Electrodes (V_{SM}) of 0.75-cm Radius at Negative Potential 46

22. Ratios of Breakdown Voltages for 2-C_4F_6/N_2 Mixtures with Rough (grooved) Inner Electrodes (V_R) and with Smooth Electrodes (V_{SM}) of 0.75-cm Radius at Positive Potential 47

23. Ratios of Breakdown Voltages for 2-C_4F_6/N_2 Mixtures with Rough (grooved) Inner Electrodes (V_R) and with Smooth Electrodes (V_{SM}) of 0.75-cm Radius at Negative Potential 48

24. Breakdown Voltages of SF_6/N_2 Mixtures and Fluorocarbon/N_2 Mixtures in the Presence of Copper Wire Particles with 0.75-cm Radius Inner Electrodes at Positive Potential 53

25. Breakdown Voltages of SF_6/N_2 Mixtures and Fluorocarbon/N_2 Mixtures in the Presence of Copper Wire Particles with 0.75-cm Radius Inner Electrodes at Negative Potential 54

CHAPTER I

INTRODUCTION

In a gas under an electric field, the free electrons in the gas have a distribution of energies extending over a wide range. These free electrons are responsible for the formation of an avalanche, which may lead to a breakdown. By controlling both the number and energies of these free electrons in the gas, breakdown can be inhibited (1,2).

In this research, knowledge of fundamental electron-molecule interactions has been applied to the design of good gaseous dielectrics in DC practical systems. The first basic idea is to attach the free electrons in a gas to the gas molecules to form negative ions which are too large and too slow to initiate breakdown. Since the electron attaching and slowing-down properties of a dielectric gas are functions of electron energies, and since different gas molecules possess different abilities to capture electrons, it is believed that the best dielectrics should be multicomponent gas mixtures which can provide larger attachment cross sections over a wider energy range than any single gas does (1,2). However, all attachment is limited to fairly low energies. The second basic idea is then to use other molecules to guard the energy range above which appreciable attachment occurs. To achieve this, an electron thermalizing gas is mixed with an electron attaching gas so that electrons with energies above the attachment range are returned to the lower energy range for

efficient capture. Nevertheless, the attaching gas and the thermalizing gas should be chosen as a team, i.e. their cross sections should cover different but closely adjacent energy ranges.

In these experiments, four binary mixtures (SF_6/N_2, c-C_4F_8/N_2, 2-C_4F_8/N_2, and 2-C_4F_6/N_2) have been analyzed. Basically, these binary mixtures contain one electron-attaching gas and one electron-thermalizing gas. The electron-attaching gases are SF_6 (sulfur hexafluoride), c-C_4F_8 (perfluorocyclobutane), 2-C_4F_8 (perfluorobutene-2), and 2-C_4F_6 (hexafluoro-2-butyne). The availability and cost of these electron-attaching gases are listed in Appendix I. The electron-thermalizing gas is N_2. The attaching gases serve as an additive to N_2 from 0% to 100% at a total pressure of one atmosphere.

The breakdown results of fluorocarbon mixtures were compared with SF_6 mixtures and were found to be superior to SF_6 in every aspect. This is due to the fact that SF_6 has a large electron attachment cross section at low energies ($\lesssim$ 0.4eV), but is unable to attach any electrons appreciably beyond this energy range. On the other hand, the fluorocarbons are able to attach electrons over a much wider energy range ($\lesssim$1.2eV). The effects of surface roughness, particle contaminants and electrode materials were also studied. Thus, the breakdown data and fundamental physicochemical properties of gases can be correlated in the design of good gaseous dielectrics in practical systems.

CHAPTER II

THEORETICAL ANALYSIS

In this chapter the electrical breakdown mechanisms of gases and the control of gas breakdown by knowledge of fundamental electron-molecule interactions will be discussed. The classical Townsend theory (3,4) of the growth of ionization and the streamer theories proposed by Loeb and Meek (5) are fundamental and essential to any discussion of electrical breakdown mechanism of gases. The Townsend theory is generally accepted for the formation of a spark in a uniform field under quasistatic conditions. However, its application to a non-uniform field is very doubtful. It must be supplemented by the streamer theory in order to describe many observed phenomena which cannot be explained by the Townsend theory. The breakdown criteria from these theories will be discussed later. There are other spark breakdown criteria that deserve attention too (6,7), but in this thesis only the Townsend and the streamer criteria are discussed.

The most efficient way of inhibiting breakdown of a gas is by controlling the number of free electrons (1,2). This can be achieved by attaching the electrons to neutral molecules to form negative ions which are too heavy and too slow to gain enough energy from the electric field for ionization. Meanwhile, the electrons which have gained enough energy for ionization are slowed down by the electron thermalizing gas to the attachment energy range of the electron attaching gas.

The electron attaching and thermalizing gases must be chosen to work well together because each gas possesses different abilities to capture and slow down electrons. Also, these properties are a function of electron energy and the distribution functions of electrons are dependent on the gas itself and the applied electric field. Therefore, the optimum gas dielectric is considered to be a multicomponent gaseous system which can provide the largest attachment cross section for electrons over the widest electron energy range. The binary mixtures used in this experiment are designed by this principle with mainly one electron-attaching gas and one electron-slowing down gas.

I. ELECTRICAL BREAKDOWN MECHANISMS OF GASES

In the study of gas discharges, a knowledge of the processes leading to a spark breakdown is essential. Generally, gas discharges are divided into two types: self-sustaining and non-self-sustaining discharges. The spark breakdown mechanism of a gas is a transition from non-self-sustaining discharge to self-sustaining discharge with explosive suddenness (4). The free electrons and their distribution of energies in a gas play a very important role in any gas breakdown mechanism. These free electrons under an applied electric field gain enough energy to ionize the neutral gas molecules by collision. Thus, new electron ion pairs are produced by this cumulative process. As this process goes on, the number of ions and electrons grows very rapidly and electron

avalanches are formed. When the applied electric field increases up to a certain critical value, the number of ions and electrons increases to a point where a self-sustaining discharge is established and results in a spark breakdown.

Two types of breakdown mechanisms will be discussed in this thesis: the Townsend theory states that a succession of electron avalanches, initiated at the cathode, is essential for the build-up of a breakdown and the streamer theory states that only one single electron avalanche can lead to a breakdown.

The Townsend Theory

In the early 1900's J. S. Townsend proposed his now classical theory of the mechanism of spark discharge in gases. His theory was based upon the field-intensified ionization of the neutral molecules of a gas by electrons which started a succession of electron avalanches and eventually lead to a breakdown. A gas is normally a very good insulator, but some electrons and ions are always present due to the natural background of cosmic radiation. Under an electric field, these ions and electrons will be accelerated. The electrons, which have a much smaller mass than the ions, will be accelerated very rapidly and gain enough energy for ionization by collisions with the neutral molecules. This process is cumulative and occurs extremely rapidly.

The above process is known as the primary ionization process. There are other secondary processes which contribute to the breakdown mechanism. The most important secondary

process of ionization is caused by the positive ions. These positive ions gain considerably less energy than the electrons because of their much larger mass and thus it is very unlikely that they can ionize the neutral molecules. However, they can produce new electrons by bombardment of the surface of the negative electrode. Also, new electrons can be produced by photoionization in the gas caused by photons originated from excited atoms or from recombination processes of ions and electrons.

The current density at the anode in a nonuniform field, due to primary and secondary processes of ionization, can be expressed as (8):

$$J = J_0 \frac{1 + \int_0^d \exp\left\{\int_0^x (\alpha - \eta)\, dx\right\} \alpha\, dx}{1 - \gamma \int_0^d \exp\left\{\int_0^x (\alpha - \eta)\, dx\right\} \alpha\, dx} \qquad (2\text{-}1)$$

where J is the current density, J_0 is the initial current density due to external ionizing sources, d is the gap length, α is the number of ionizing collisions for an electron for unit length of path in the direction of the field and is called Townsend's first ionization coefficient, γ is the number of new electrons to be emitted from the cathode for each of the bombarding positive ions and is called the second Townsend ionization coefficient, and η is the electron attachment coefficient defined as the number of attachments per electron per unit length of path in the direction of the field.

This equation can determine the voltage level at which a nonuniform field gap breaks down according to the Townsend theory, because breakdown must occur when the current becomes infinite. This happens when the denominator becomes zero:

$$\gamma \int_0^d \exp\left\{ \int_0^x (\alpha - \eta)\, dx \right\} \alpha\, dx = 1 \qquad (2\text{-}2)$$

Equation (2-2) is the criterion for the Townsend mechanism of spark breakdown in an electron-attaching gas in a nonuniform field. For a uniform field α, γ and η are constants. Thus, equation (2-2) becomes:

$$\frac{\gamma \alpha}{\alpha - \eta} \left[\exp\left\{ (\alpha - \eta) d \right\} - 1 \right] = 1 \qquad (2\text{-}3)$$

Equation (2-3) is the criterion for the Townsend mechanism of spark breakdown in a uniform field.

Although the Townsend theory can predict the voltage level at which a uniform field gap breaks down, it does not give any information about the actual breakdown process and its application of the Townsend theory is restricted to quasi-static conditions.

The Streamer Theory

A new theory of spark breakdown mechanism was proposed in 1940 by Meek (9) and is generally referred to as the streamer theory. This theory is based on considerations of

a single electron avalanche, the transition from an avalanche into a streamer, and the mechanism of advance of streamers across the spark gap. According to this theory the space charge field from the electrons and ions in the head of an avalanche may cause an instability in the development of the avalanche, resulting in the formation of fast moving anode and cathode directed filamentary streamers from the avalanche head (3,5). The streamers form a highly conducting plasma channel across the gap leading to the ultimate collapse of the voltage. The basic mechanism behind the formation of streamers is thought to be photoionization in the gas.

A satisfactory quantitative physical theory for streamer formation has not yet been formulated. Meek made the assumption that cathode and anode directed streamers would develop when the radial space charge field from the ions in the avalanche head become comparable with the externally applied field. This leads to Meek's equation for the breakdown of a nonuniform gap in non-attaching gas (3,5).

$$\alpha_x \exp\left\{\int_0^x \alpha\, dx\right\} = K E_x \{x/\rho\}^{1/2} \qquad (2\text{-}4)$$

where x denotes the critical avalanche length, i.e. the length of the initial electron avalanche at the moment when it becomes unstable and streamers are formed. In nonuniform fields x may be much shorter than the gap length. α_x is the first Townsend ionization coefficient at the avalanche head, ρ is the gas density, and K is a constant.

This equation was later modified by Pedersen to include electron attachment (8):

$$\alpha_x \exp\left\{ 2 \int_0^x (\alpha - \eta)\, dx \right\} = F(x, \rho) \tag{2-5}$$

where η is the electron attachment coefficient of the gas, and the function $F(x,\rho)$ is an empirical function which can be determined from measured breakdown data in uniform fields.

Equation (2-5) can be simplified by writing in logarithmic form:

$$\frac{1}{2} \ln\{\alpha_x\} + \int_0^x (\alpha - \eta)\, dx = f(x, \rho) \tag{2-6}$$

It has been shown that in SF_6 $f(x,\rho)$ (10) varies little with x and ρ, and that the contribution of the logarithmic term in (2-6) (11) to the value of $f(x,\rho)$ is almost constant. Equation (2-6) may simply be written as:

$$\int_0^x (\alpha - \eta)\, dx = K \tag{2-7}$$

where K is a constant. K is dependent on the gas and is equal to 10.5 for SF_6 and about 20 for air at atmospheric pressure.

Equation (2-7) is known as the streamer breakdown criterion for SF_6. It can be interpreted as meaning that breakdown occurs when the total number of electrons in an avalanche reaches a certain value (about 10^8) (10).

II. PREVENTION OF BREAKDOWN OF GASES BY ELECTRON-MOLECULE INTERACTIONS

As discussed above, the free electrons in a gas are responsible for the formation of electron avalanches leading to a Townsend or streamer-type breakdown. Therefore, no matter what theory is followed, one effective way to prevent breakdown is the removal of these electron before they attain enough energy for ionization. An effective way to remove these electrons is to attach them to molecules forming negative ions which are too heavy to accelerate appreciably under an electric field and thus cannot attain enough kinetic energy to cause ionization. At the same time, the electrons which have escaped attachment and have gained energy high enough for ionization must be slowed down. The above statements can be formulated as (1):

$$\int_0^\infty \sigma_a(\varepsilon)\, f(\varepsilon, E/p)\, d\varepsilon \longrightarrow \text{maximum} \tag{2-8}$$

$$\int_I^\infty \sigma_i(\varepsilon)\, f(\varepsilon, E/p)\, d\varepsilon \longrightarrow \text{minimum} \tag{2-9}$$

where σ_a and σ_i are the electron-attachment and electron-impact ionization cross sections respectively, and $f(\varepsilon, E/p)$ is the electron energy distribution function as a function of electron energy and pressure reduced electric field, and I is the ionization threshold energy.

To maximize (2-8), $\sigma_a(\varepsilon)$ should be as large as possible over as wide an energy range as possible and $f(\varepsilon, E/p)$ must be

shifted to as low energies as possible because all attachment is limited to lower energies. To minimize (2-9), $\sigma_i(\varepsilon)$ should be as small as possible, I should be as high as possible, and $f(\varepsilon, E/p)$ must be shifted to as low energies as possible. Thus, the reduction of electron energies in a gas is very important because a lower $f(\varepsilon, E/p)$ can optimize both (2-8) and (2-9). However, the electron attachment cross section $\sigma_a(\varepsilon)$ plays a dominant role in the dielectric strengths of gases. As a result, the electron impact ionization cross section $\sigma_i(\varepsilon)$ is not so important in designing good gaseous dielectrics (12,13,16, 18,19). The electron energies can be reduced by elastic and inelastic electron scattering, especially in the subexcitation energy range. One efficient way of slowing down subexcitation electrons is via negative ion resonance (NIR). The figure on page 15 shows the vibrational excitation cross sections via NIRs for CO, N_2, and H_2. NIR states can be positioned over the entire subexcitation energy range through a proper combination of gases so that electrons in this energy range can be slowed down.

Therefore, the optimum gaseous dielectric is considered to be a combination of gases which are chosen to provide the best electron-attaching and electron slowing-down properties to optimize (2-8) and (2-9) (1). This can be achieved by a knowledge of physicochemical properties of the gases and fundamental electron-molecule interactions.

Electron Attachment of Dielectric Gases/Mixtures as Functions of Electron Energy

Figure 1 (12) shows the electron attachment cross section versus electron energy for four electronegative gases: SF_6, c-C_4F_6, 2-C_4F_8, and 2-C_4F_6. The electron attachment cross section $\bar{\sigma}$ of a gas, together with its number density N, gives the probability that a fundamental electron-molecule interaction (attachment) will occur. Therefore, the larger the attachment cross section, the higher is the probability of electron attachment. The size of the electron attachment cross section is not the only way to predict the dielectric strength of a gas. The electron energy range over which effective attachment is possible is also a very important factor. As can be seen in Figure 1, the electron attachment cross section is a function of electron energy.

In Figure 1, SF_6 has a large attachment cross section at $\lesssim$ 0.4 eV. Electrons beyond this energy range will escape attachment and accelerate under the electric field and eventually cause ionization. The fluorocarbons have a much wider energy range for electron attachment, with 2-C_4F_6 at $\lesssim$ 1.2eV and both 2-C_4F_8 and c-C_4F_8 at $\lesssim$ 1.0eV. Therefore, the fluorocarbons are expected to have higher dielectric strength than SF_6 as will be proved in the experimental analysis chapter. The dielectric strengths of these four gases decrease in the order 2-C_4F_6, 2-C_4F_8, c-C_4F_8, and SF_6.

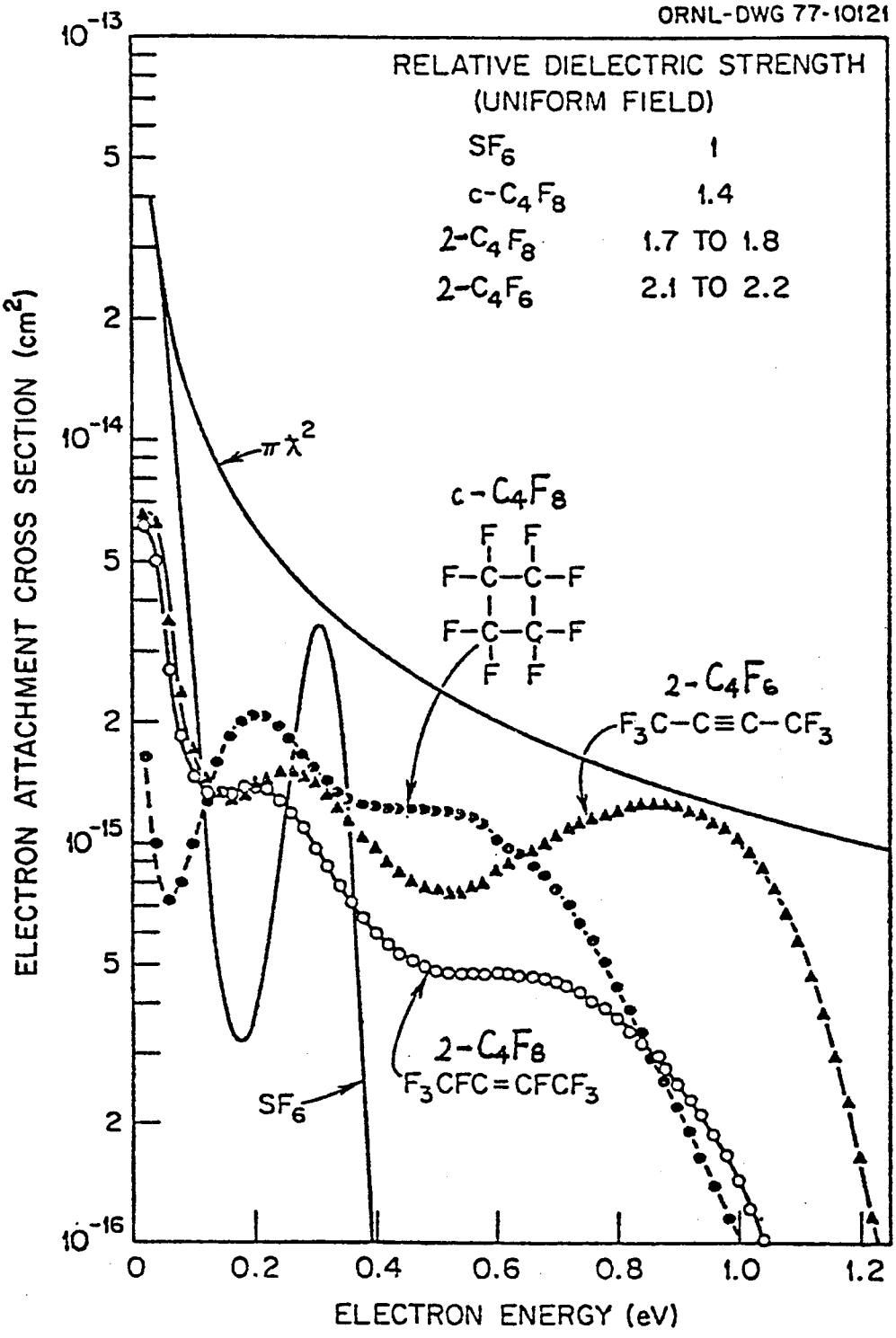


Figure 1. Electron attachment cross section versus electron energy for 2-C_4F_6, c-C_4F_8, 2-C_4F_8, and SF_6. $\pi\lambda^2$ is the maximum s-wave electron capture cross section (1).

Electron Slowing-Down Properties of Dielectric Gases/Mixtures as Functions of Electron Energy

Figure 2 (13,14) shows the vibrational excitation cross sections of CO , N_2, and H_2 via negative ion resonances. These are electron thermalizing gases. In this thesis only N_2 is used as an electron slowing-down gas. Like the attachment cross sections, the vibrational excitation cross sections are also functions of electron energy. N_2 is a fairly good electron slowing-down gas because it has a large vibrational excitation cross section from $\sim$ 1.8eV to $\sim$ 3.4eV. This means that N_2 is capable of slowing down electrons within this energy range.

In Figure 1 2-C_4F_8 and c-C_4F_8 have about the same electron energy range for attachment and generally c-C_4F_8 has larger attachment cross sections than 2-C_4F_8, but 2-C_4F_8 has a higher dielectric strength. This is due to the presence of the double bond in 2-C_4F_8 (15,16) which is very effective in inelastic scattering and contributes significantly in slowing-down electrons.

In this research, the dielectric strengths of four binary mixtures which contain one electron attaching gas and one electron slowing-down gas, have been studied in practical systems. The experimental analysis and results will be presented in the next chapter.

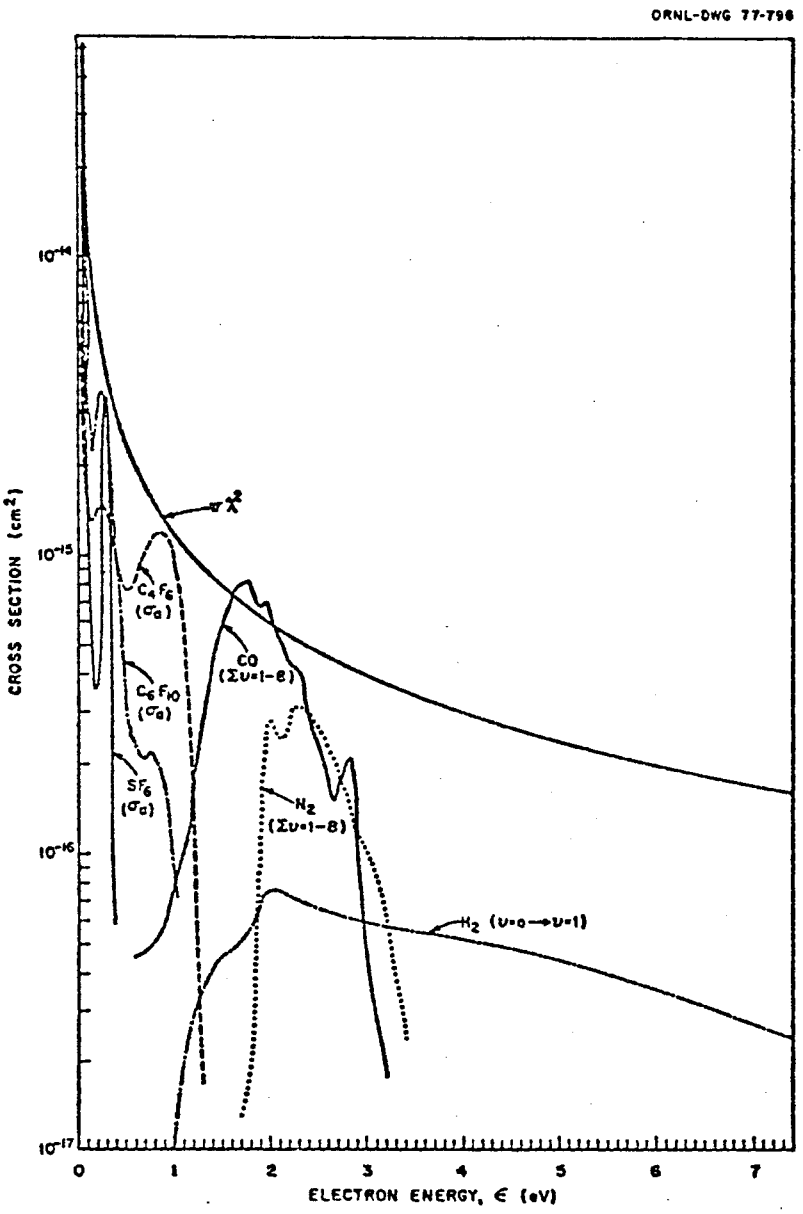


Figure 2. Vibrational excitation cross sections versus electron energy for N_2.

CHAPTER III

EXPERIMENTAL ANALYSIS

In this chapter the breakdown strengths of the attaching gases/N_2 mixtures are evaluated in practical systems. Figure 3 and Figure 4 show the facility used for breakdown strength measurements. The equipment is divided into two major parts. One is the high voltage part of the equipment which is inside a wire mesh shielding cage. The other is the controlling part which is outside the shielding cage. The purpose of this arrangement is to shield the r.f. noise generated by the spark breakdown of the gases so that the excessive noise effects on the instrumentation can be eliminated.

Three sets of concentric cylinder electrodes of different inner sizes have been built and used in breakdown tests. These electrodes are mounted horizontally in a high vacuum chamber filled with the gas. Breakdown strength measurements have also been made on concentric cylinder electrodes with two degrees of roughness and three different electrode materials. Finally, particles are introduced into the systems to study their behavior under nonuniform electric field and their effects on the dielectric strengths of gases. The apparatus and experimental procedure will be described in more detail in the following sections.

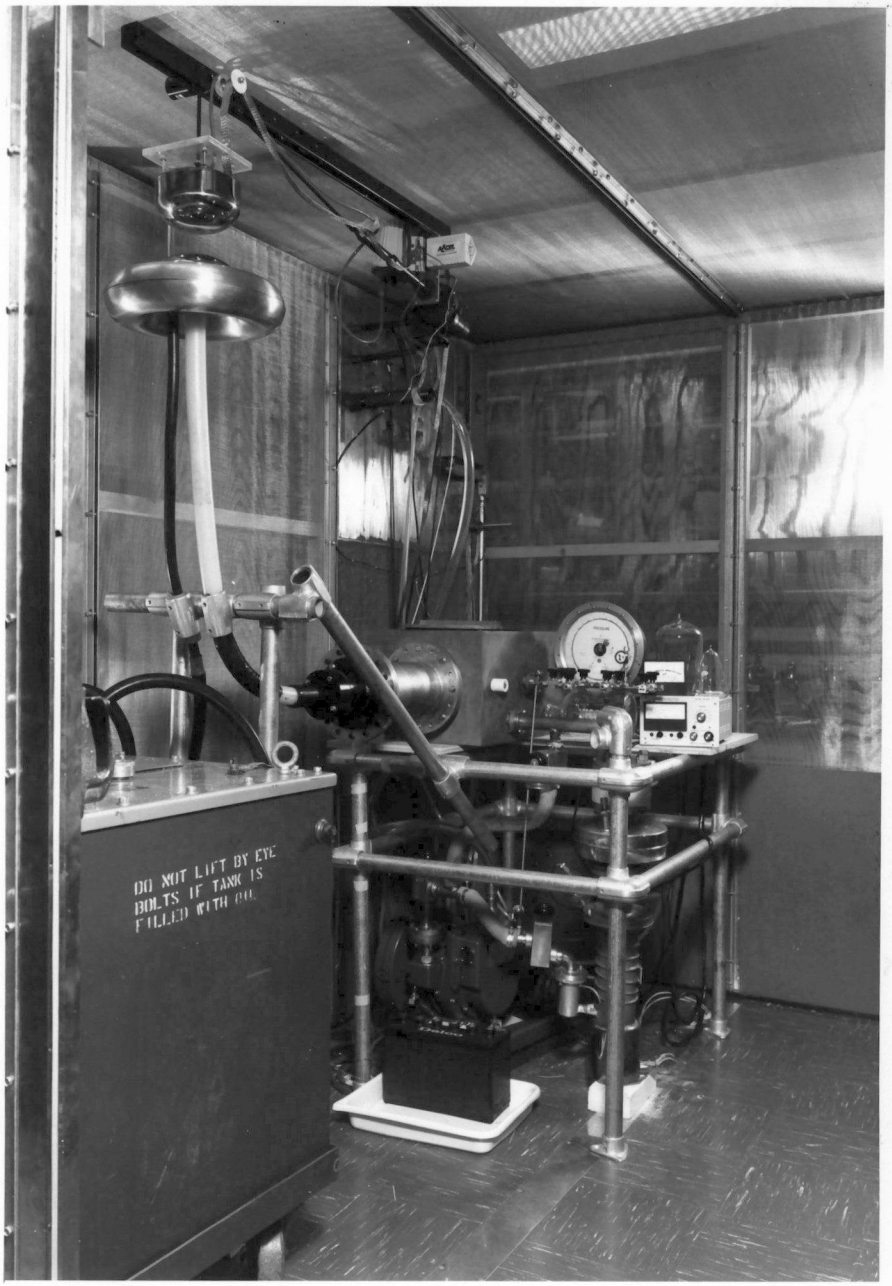


Figure 3. Interior of shielding cage of cylindrical electrode facility.

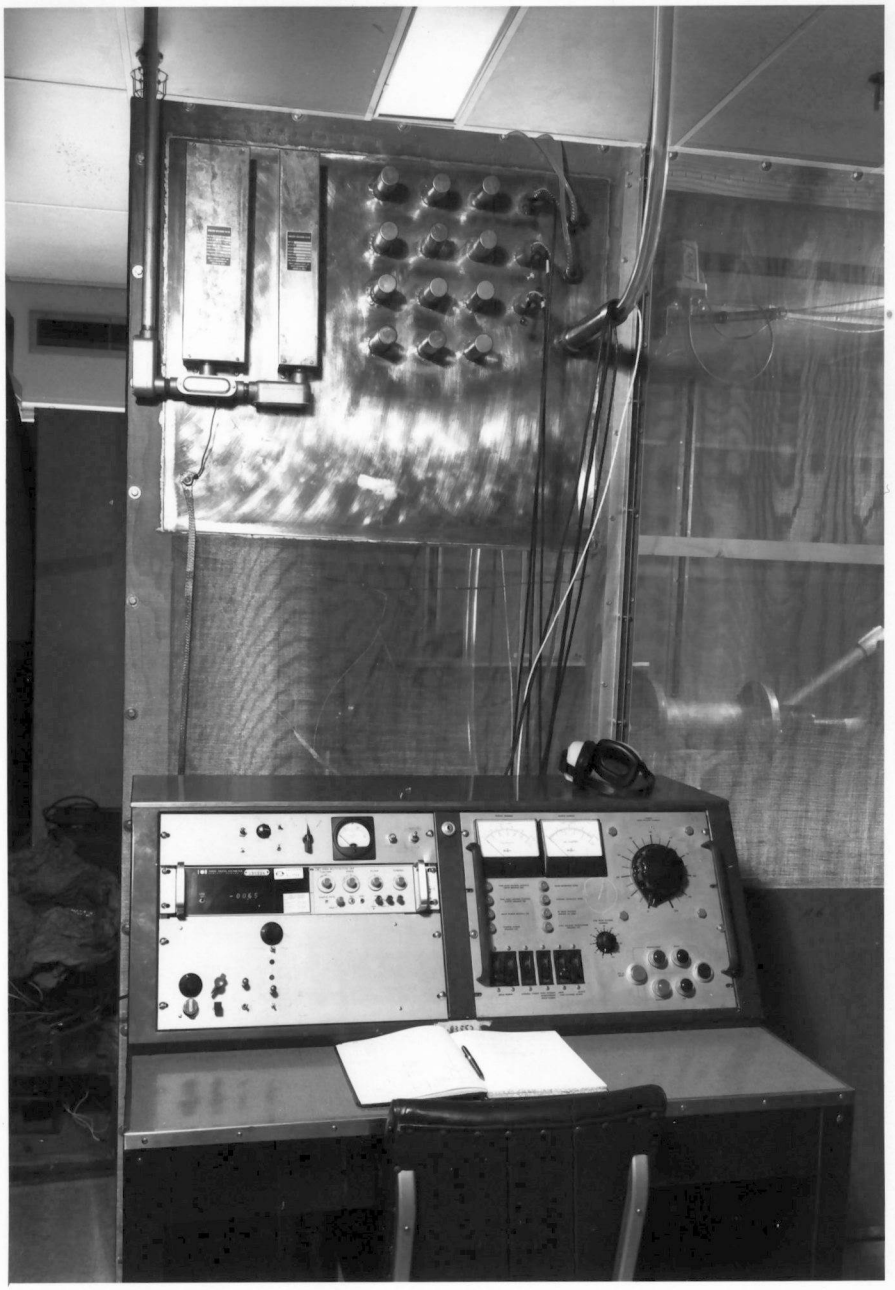


Figure 4. Exterior view of the shielding cage of cylindrical electrode facility.

I. EXPERIMENTAL APPARATUS

Three major pieces of apparatus are essential to the experiments, namely the chamber, the electrodes, and the electrical system of the apparatus. With these apparatuses, gases/mixtures are tested under conditions simulating those in power applications. The results are correlated with basic physicochemical properties of the gases/mixtures for the future engineering design of practical power apparatus.

Chamber

The chamber is a 2.5'x1'x1' rectangular box and has a volume of approximately 60 litres. It is designed to operate at low pressure (approximately one to two atmospheres). In order to save the expensive gases/mixtures, roughly 20 litres are occupied by sealed glassware. The chamber has several gas, optical and electric ports on each side. There is a 2-inch-diameter quartz window facing the rear cage wall and a 7"x4" rectangular plexiglas window on the top cover. Ultraviolet light from a 60-watt deuterium lamp can be directed onto the inner cylinder through the quartz window via a partially reflecting, partially transmitting mirror made by vacuum deposition of aluminum such that full view is made possible through the window. This is very vital to the particle contaminant studies because the characteristic motions of particles can be observed directly through this window. The chamber is also fitted with a mechanical forepump, a diffusion pump, a liquid nitrogen trap and appropriate valves and gauges.

It receives high voltage via a cable feedthrough of the type used at the output of Delta Ray Corporation power supplies.

Electrodes

The concentric cylinder electrodes are shown in Figures 5 and 6. The outer cylinder was machined with smoothly tapered ends from a solid brass block to effect a cylinder of 2-cm inner radius and a 10-cm length of central cylinder, plus 11-cm length of tapered ends. Seven inner cylinders of 27-cm length and radii 0.4, 0.75, and 1.4 cm have been made (see Figure 7). The 1.4-cm radius cylinders are made of three materials (stainless steel, copper, and aluminum). The 0.75-cm radius cylinders have three degrees of roughness (smooth, 0.004" spiralling grooves and 0.02" spiralling grooves). The inner electrode is held at the ends and is centered within the outer electrode by plexiglas bushings. The inner electrode is connected to the high voltage power supply by a rod screwed into it. The outer electrode is connected to a one megohm resistor string, and to a 50-KV bushing in the chamber wall with electrical connection to ground made outside the chamber through small current-sensing resistors.

The electric field at the surface of the inner cylinder between two infinitely long concentric cylinders is given by:

$$E = \frac{V}{r_1 \ln(r_2/r_1)} \qquad (3\text{-}1)$$



Figure 5. Outer electrode assembly for concentric cylinder electrode geometry.



Figure 6. Mounted concentric cylinder electrodes.



Figure 7. Inner electrodes for concentric cylinder geometry.

where V is the voltage applied between the cylinders, r_1 and r_2 are the radii of the inner and outer cylinders respectively. By taking the partial derivative of E with respect to r_1 for a constant r_2 and setting $(\partial E/\partial r_1) = 0$. The minimum E field can be found when $r_2/r_1 = e$ (the basis of natural logarithms). The radii of the electrodes are designed according to the following ratio approximately: 0.5e, e, and 2e. Since the E field at r_1 is minimum when the ratio of outer and inner radii is e, the 0.75-cm radium cylinder is expected to have the highest breakdown voltages. Also, the field fringing effects at the open ends of the electrodes weaken the electric field at the central region. As a result, the 0.4-cm electrode which has the largest fringing effects, has slightly higher breakdown voltages than expected relative to the others. These effects will be verified later.

Electrical System of Apparatus

The power supply provides zero to ±150-KV DC with ripple less than 0.1%. It consists of an oil tank in which high voltage components are submerged and a rack on which the low voltage controls are mounted outside the cage. Positive or negative polarity can be selected by a switch submerged in the oil tank. Two high voltage vacuum diodes in the oil tank form a voltage-doubler circuit, charging two 0.006-μF capacitors in series. It also provides a 300-MΩ resistor string in series with a 300-MΩ resistor string to form a voltage divider. A digital voltmeter (Hewlett-Packard 3480D) is

connected in parallel with the 300-KΛ resistor to sample the high voltage output. A Spelman power supply is used to calibrate this voltmeter.

The controller circuit generates a rising ramp waveform at a slow, controlled rate beginning from some selected "base" voltage below breakdown. A feedback circuit compares the voltage divider output with the ramp signal and operates a motor-driven variable transformer according to the error signal, making the high voltage follow the ramp waveform. Breakdown is sensed by ground electrode current. The digital voltmeter is used to acquire the breakdown voltages. This voltmeter samples the output of the 1000:1 divider at a rate of approximately twenty times per second. When a breakdown is detected, the controller circuit commands the digital voltmeter to hold the last voltage reading just before the breakdown, while the high voltage is rapidly returned to the lower "base" value. A timer in the controller holds the breakdown voltage for a preset time for recording and recycles the measurement process.

A diverter gap is connected across the HV line between the power supply output and the test gap. The diverter consists of a pair of 6-inch-diameter stainless steel hemispheres, one at high voltage and backed by a corona shield and one at ground potential and fitted with the trigger electrode. This trigger electrode consists of 1/8-inch-diameter tungsten rod inside a 5/16-inch-diameter quartz rod. The diverter-ground electrode is suspended from the cage ceiling by a chain driven

by a linear actuator motor/gear set so that the gap can be adjusted from outside. The trigger is activated by a 50-KV pulse from a high performance auto-ignition system mounted at the ceiling adjacent to the gap-adjustment motor. Within microseconds after a breakdown, the diverter spark gap is triggered to reduce the energy of the breakdown arc across the test gap so that the possibility of pitting the test electrodes is minimized.

A copper mesh shielding cage is used to surround the chamber, diverter and the high voltage parts of the power supply to protect the instrumentation from the RF radiation of spark breakdown. All electrical connections for power and instrumentation inside the cage are made via capacitive feed-through filters mounted through the cage wall. Water and gas exhaust connections are also carried through the cage walls by wave guides. They are all visible over the chamber as shown in Figures 3 and 4 (see pages 17 and 18).

II. EXPERIMENTAL PROCEDURE AND TECHNIQUES

To begin the experiment, the chamber is first pumped out to a high vacuum (approximately 10^{-6} torr) by the mechanical forepump and an oil diffusion pump with liquid nitrogen trap. An ion gauge and a thermocouple gauge are used to monitor the vacuum pressures. When a desired low pressure is reached, the valves to the diffusion pump and mechanical forepump are closed. Test gases/mixtures are then introduced into the chamber according to the measured partial pressures of the

components. The chamber pressure is monitored by a Wallace and Tiernan FA-145 pressure gauge.

High voltage is applied between the electrodes by following the ramp signal generated by the electronic controller at a slow controlled rate, beginning from some selected "base" voltage below breakdown. At the same time, the gap is illuminated by ultra violet light to produce free electrons which are essential to initiate breakdown conditions. When breakdown occurs, a surge of current is produced in the ground electrode lead. This current is sensed by a detector which sends a signal to the electronic controller. The controller then commands the digital voltmeter to hold the last voltage reading just before the breakdown and rapidly returns the high voltage to the "base" value. The breakdown voltage is recorded and the measurement process recycles again. At least ten breakdown measurements are made for each breakdown voltage. The mean of these breakdown measurements is generally within a random scatter (standard deviation ÷ mean x 100) of less than 3%. However, with particles between the electrodes, the scatter is between 5% to 10%.

When breakdown measurements of a certain gas/mixture are finished, the electrodes are taken from the chamber to be checked for deposits and to be cleaned. Acetone is first used to clean the deposits and then methanol is used to remove the trace left by acetone. The electrodes are reinstalled for another gas/mixture and the same measurement process is repeated.

Some modifications to the practical system have to be made in studying the particle contaminant effects. Particles tend to bounce to a low field region under an electric field. Therefore, they bounce to the open ends of the ground electrode and escape from the system. Two hollow Lexan discs have been installed at the open ends of the ground electrode to stop the particles from bouncing out of the system. Unfortunately, the particles sometimes get stuck to the Lexan discs and cause a breakdown, burning a track along the discs. As a result, the inner and outer cylinders become short-circuited. Direct observation of particle activities eliminates the possibilities of tracking the Lexan discs. When particles are stuck, high voltage is immediately lowered and then raised very rapidly. Eventually, the sudden increase of electric field will "shake" the particles loose. This method of getting the particles free has been very satisfactory.

III. BREAKDOWN RESULTS

The breakdown voltages of SF_6/N_2 mixtures and three fluorocarbon gases/N_2 mixtures measured in DC practical systems are presented in the following sections. One very significant result is that all three fluorocarbons are proved to be better dielectrics than SF_6 just as predicted in chapter two, especially 2-C_4F_6 which possesses the highest dielectric strength among all other gases. Also, 2-C_4F_6 is extremely effective as an additive to N_2. It should be noted that SF_6 works particularly well with N_2 and exhibits a synergistic

effect in N_2. This phenomenon will be explained later in terms of electron-molecule interactions. Finally, the results of these experiments are correlated with the electron attachment cross sections and electron slowing-down properties of these gases as a function of electron energy in the design of gaseous dielectrics.

The Breakdown of Gases/Mixtures Between Smooth Electrodes

The breakdown voltages for mixtures of SF_6/N_2, $c\text{-}C_4F_8/N_2$, $2\text{-}C_4F_8/N_2$, and $2\text{-}C_4F_6/N_2$ between three different sets of smooth concentric cylinder electrodes (with stainless steel inner cylindrical electrodes of 1.4, 0.75, and 0.4 cm radii) for both inner-cylinder polarities are presented in Figures 8, 9, 10, and 11 respectively (17). The breakdown data of uniform field obtained from other experiments performed at Oak Ridge National Laboratory (12,13,16,18,19) are also given. The uniform breakdown curve has been normalized to each point for pure N_2 with negative polarity so that comparison can be made of the shapes of the breakdown curves in uniform and nonuniform fields. The error bars in Figure 8 to Figure 11 show combined estimated systematic and observed random errors. The observed random error is defined as standard deviation ÷ mean of at least ten observations and is less than 3% for each plotted data point.

In Figure 8 the breakdown voltage data of SF_6/N_2 are characterised by its saturation effect due to the fact that SF_6 has a large attachment cross section only at electron energy below 0.4eV (see Figure 1 on page 13). Any electrons with

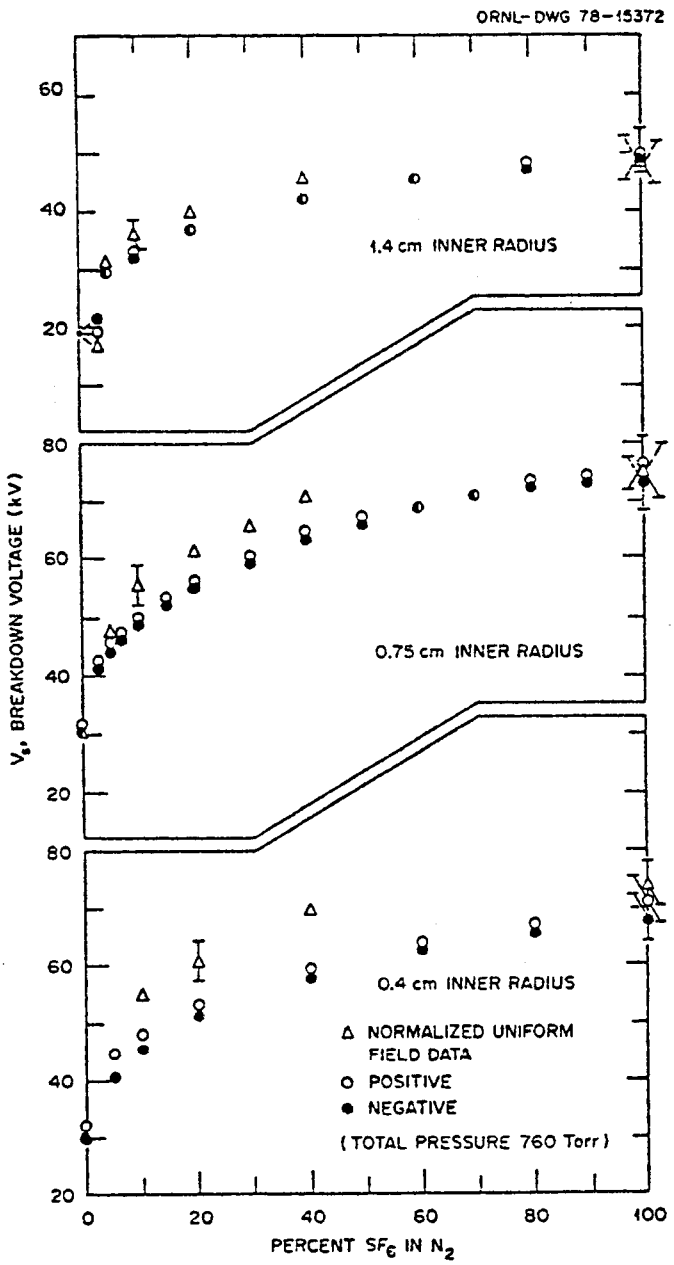


Figure 8. Breakdown voltages for SF_6/N_2 mixtures with smooth inner electrodes.

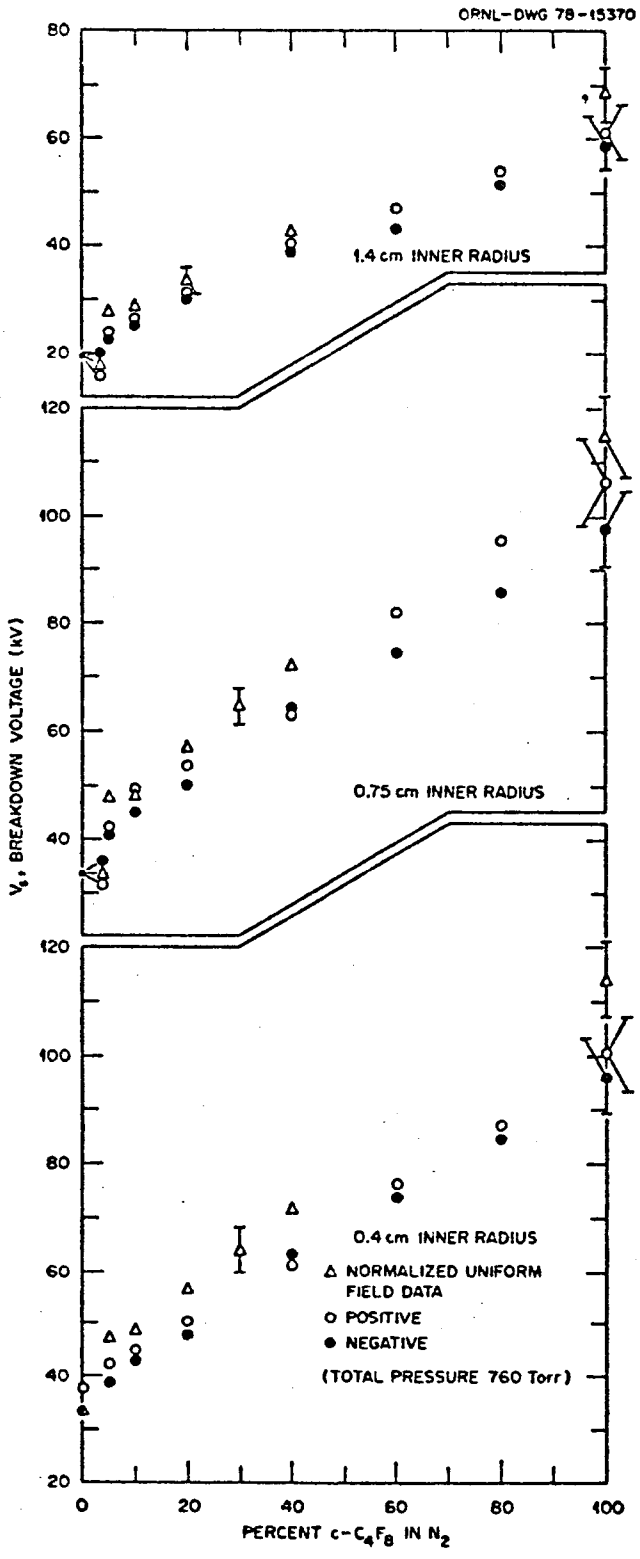


Figure 9. Breakdown voltages for c-C_4F_8/N_2 mixtures with smooth inner electrodes.

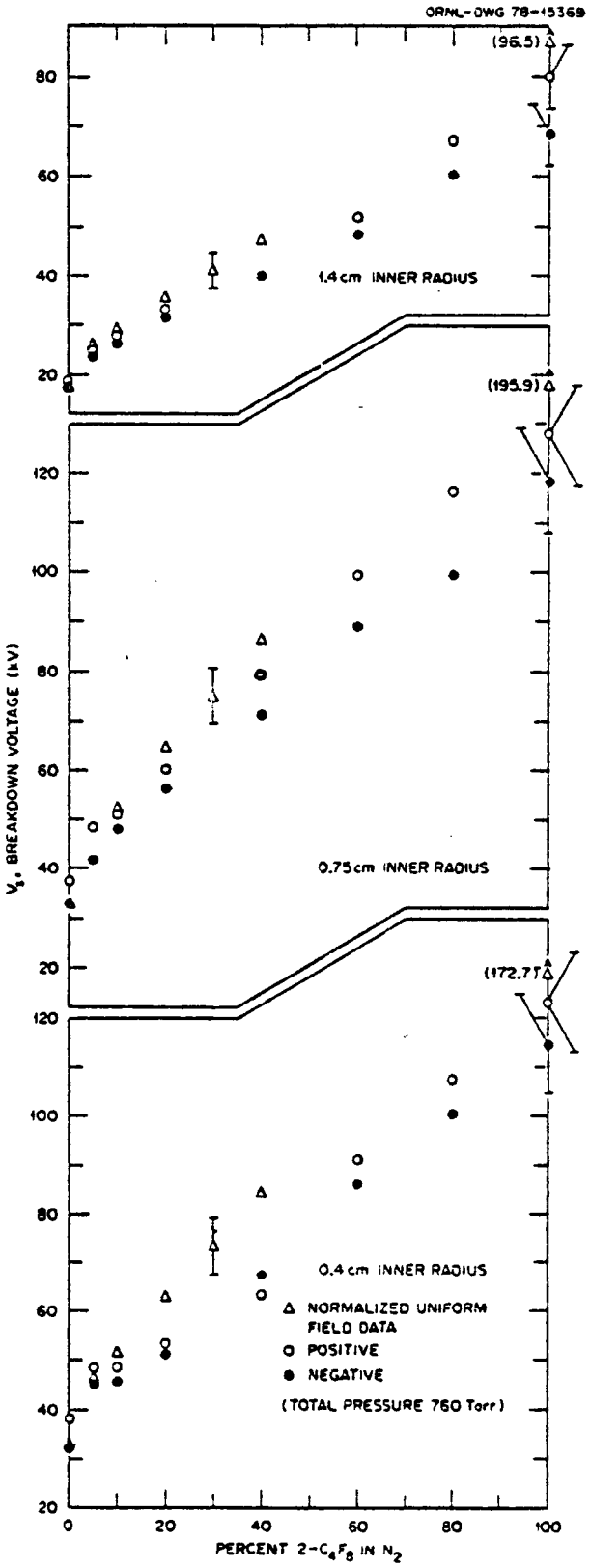


Figure 10. Breakdown voltages for 2-C_4F_8/N_2 mixtures with smooth inner electrodes.

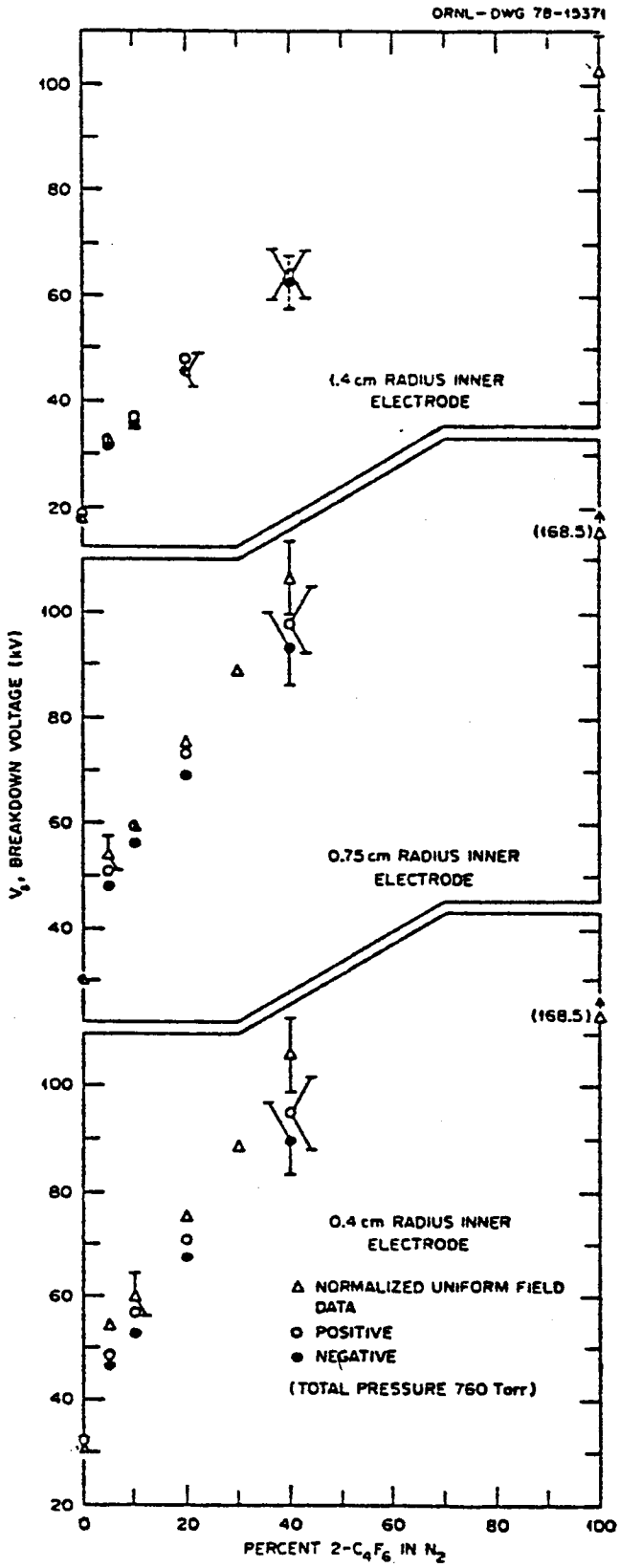


Figure 11. Breakdown voltages for 2-C_4F_6/N_2 mixtures with smooth inner electrodes.

energy higher than 0.4eV cannot be captured by SF_6 efficiently, and as a result, the addition of more SF_6 does not help much in attaching these electrons above 0.4eV. Electrons can be slowed down by inelastic scattering via negative ion resonances (NIR). Vibrational excitation cross sections for N_2 due to NIRs were shown in Figure 2 on page 15. Electrons with energies just above those where SF_6 attaches are slowed down substantially by the nitrogen molecules via NIRs so that efficient capture of these electrons is possible by SF_6.

The breakdown results of fluorocarbon/N_2 mixtures are shown in Figure 9 through Figure 11. As predicted in Chapter II, the breakdown strengths of all fluorocarbon gases are higher than SF_6 and their breakdown voltage curves are always nearly a straight line. These indicate that fluorocarbons do not work so well as SF_6 when mixed with N_2 even though they possess better dielectric strengths. The breakdown strengths of the gases decrease in the order 2-C_4F_6, 2-C_4F_8, and c-C_4F_8, and SF_6. This can be explained by looking at Figure 1 on page 13 where 2-C_4F_6 has the widest energy range for electron attachment ($\lesssim$ 1.2eV) while SF_6 has the smallest energy range. 2-C_4F_8 has only a slight margin of electron energy range ($\lesssim$ 1.0eV) over c-C_4F_8 for electron attachment, but the double bonding in its chemical structure makes it very effective for inelastic scattering and thus slows down the electrons for attachment. In other words, the higher dielectric strength of 2-C_4F_8 is attributed to its superior electron slowing-down properties as compared with c-C_4F_8.

Comparison of the breakdown curves indicates that SF_6 is more sensitive to the degree of field non-uniformity than the other gases as the cylinder field goes gradually non-uniform from 1.4 to 0.4 cm inner cylinder radius. Also, it can be seen that the breakdown voltages on the 0.75-cm radius electrode are higher than the other electrodes. This is because this electrode provides the minimum electric field at the inner electrode surface. The 0.4-cm radius electrode has breakdown voltages almost as high as the 0.75-cm radius because of more field fringing at the open ends of the smaller inner electrodes. Finally, the breakdown curves show that almost all positive breakdown voltages are higher than negative breakdown voltages. This is attributed to the fact that an electron avalanche generally begins at the cathode.

The Effects of Surface Roughness

Three 0.75-cm radius electrodes are employed to study the effects of surface roughness. Each electrode has a different degree of surface roughness:

1. Smooth all over.

2. Smooth but with a 0.004-inch deep groove spiralled around a 2-inch length in the central electrode region.

3. Same as number two except that the grooves are 0.02-inch deep.

The breakdown curves of Figures 12 to 15 (17,18,19) show the same general characteristic as the smooth electrode except the breakdown voltages are somewhat lower, depending on the

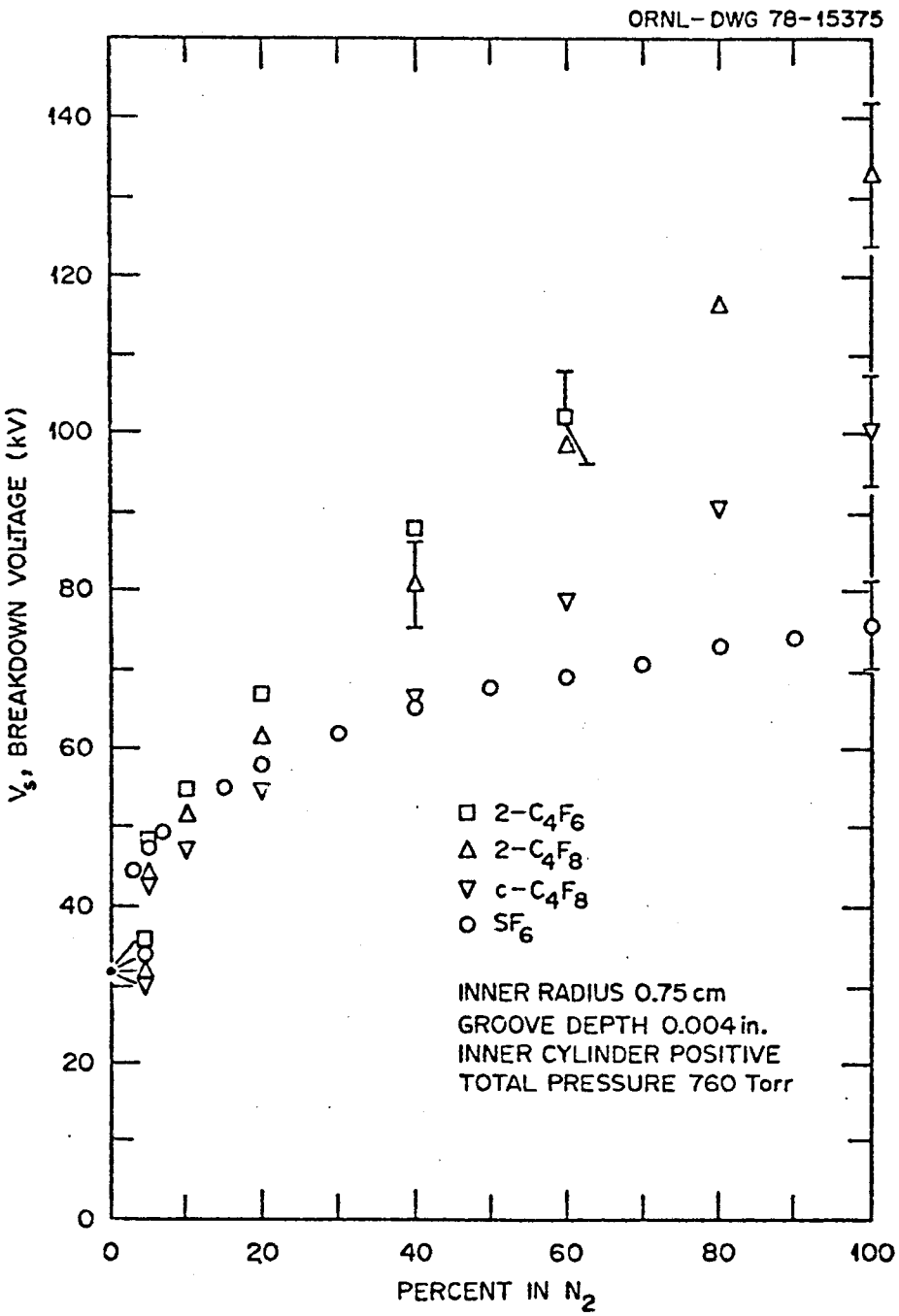


Figure 12. Breakdown voltages for SF_6/N_2 and fluorocarbon/N_2 mixtures with 0.75-cm radius inner electrode and 0.004-in. groove depth at positive potential.

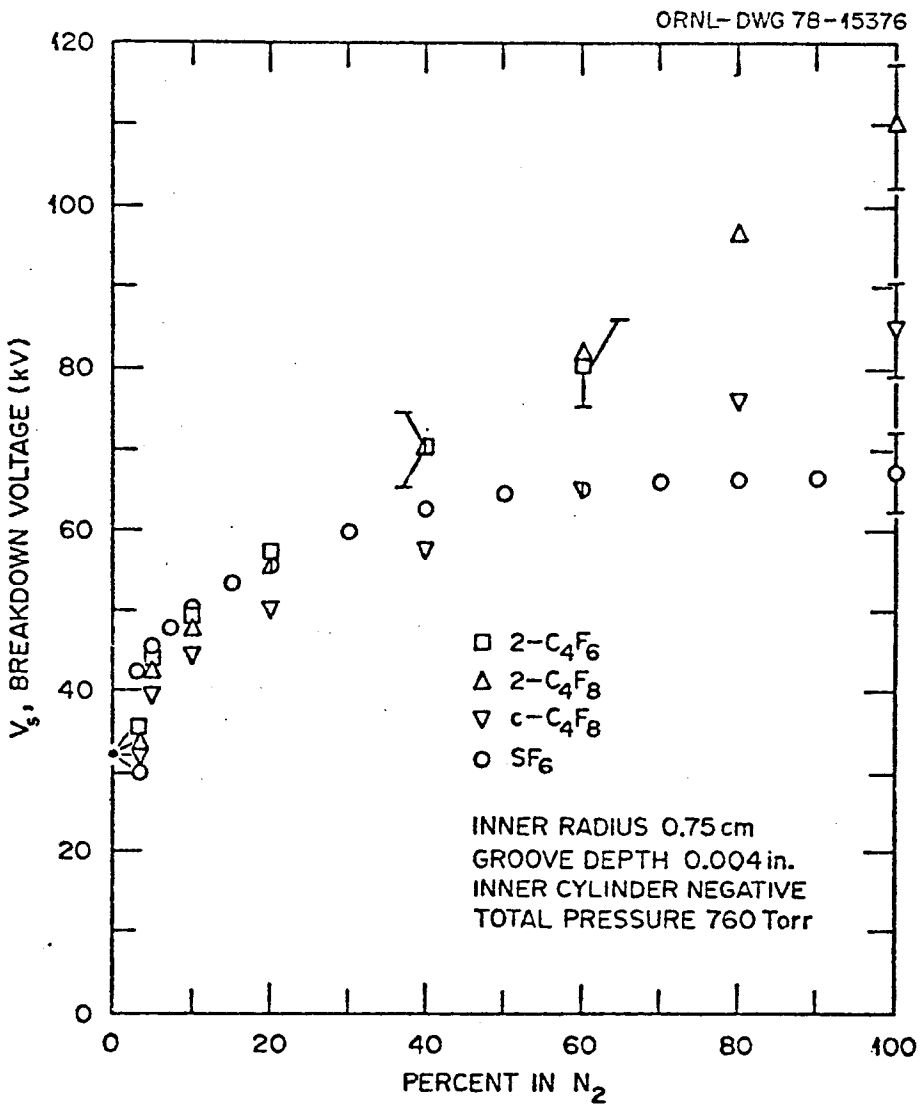


Figure 13. Breakdown voltages for SF_6/N_2 and fluorocarbon/N_2 mixtures with 0.75-cm radius inner electrode and 0.004-in. groove depth at negative potential.

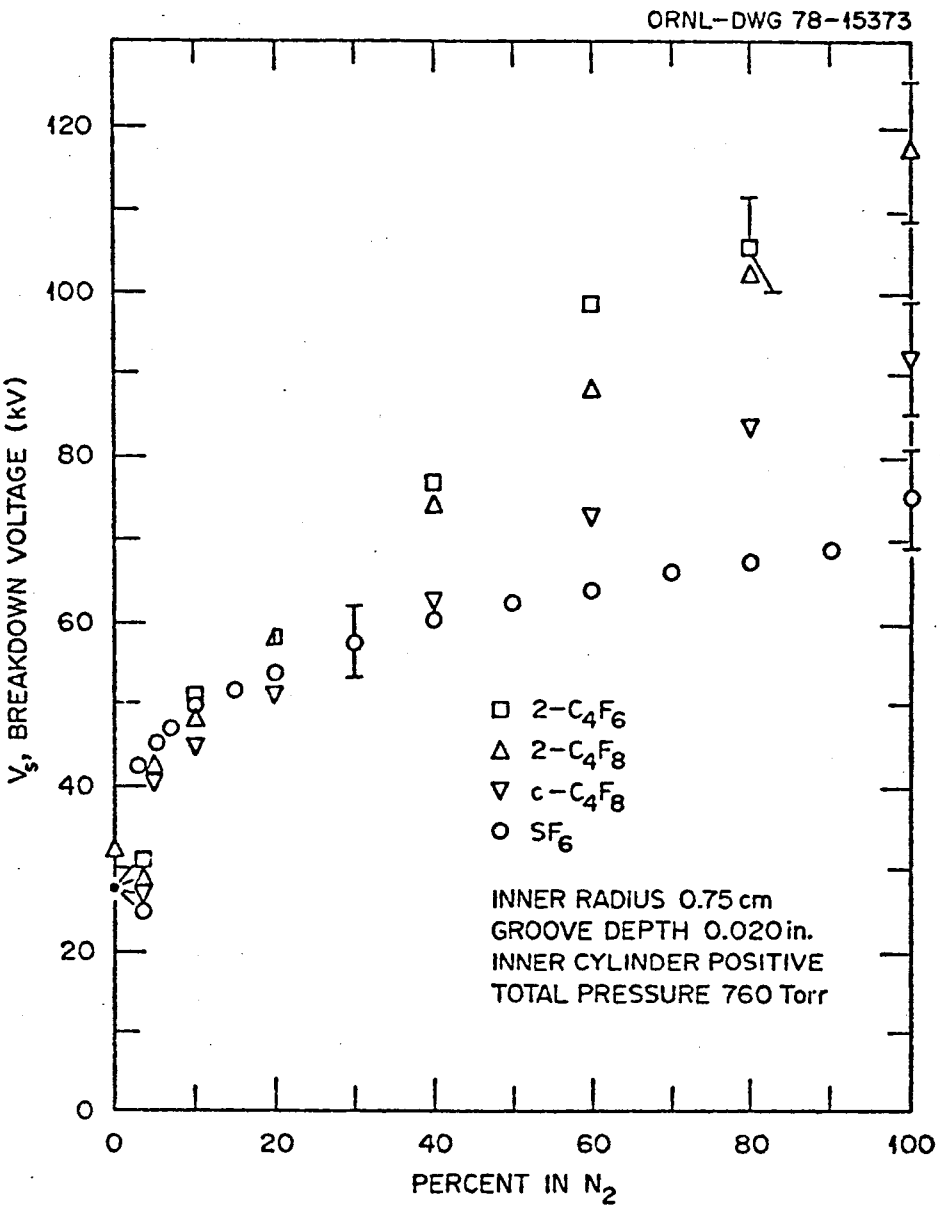


Figure 14. Breakdown voltages for SF_6/N_2 and fluorocarbon/N_2 mixtures with 0.75-cm radius inner electrode and 0.020-in. groove depth at positive potential.

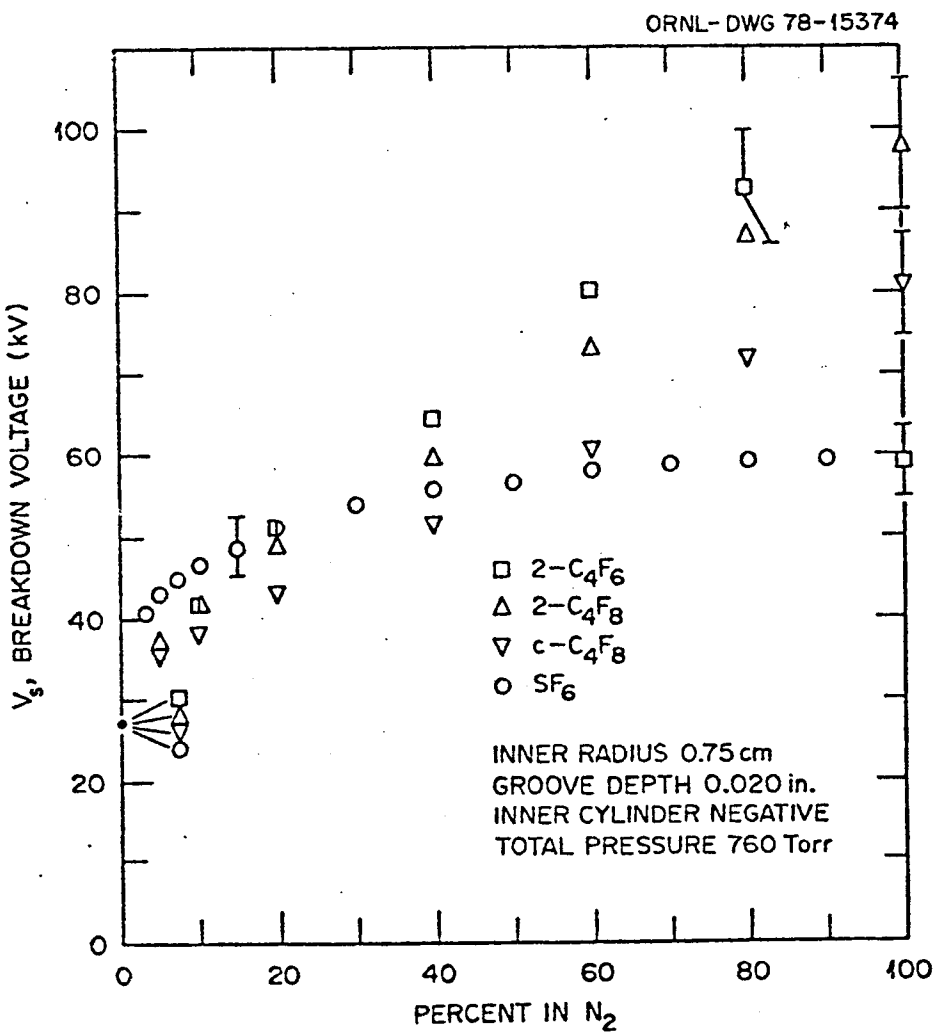


Figure 15. Breakdown voltages for SF_6/N_2 and fluorocarbon/N_2 mixtures with 0.75-cm radius inner electrode and 0.020-in. groove depth at negative potential.

degree of surface roughness. The saturation effect of SF_6 is still very obvious and the breakdown curves of fluorocarbons are still always in a straight line. In order to compare the breakdown voltages of surface roughness to those with smoothness, the ratios of these voltages are plotted in Figures 16 to 23. In these figures, V_R is the breakdown voltage with surface roughness and V_{SM} is the breakdown voltage of the smooth electrode. The degrees of roughness do affect the breakdown voltages; as can be seen that the electrode with deeper grooves lowers the breakdown voltages more than the electrode with less roughness. The results indicate that all fluorocarbons are still superior to SF_6 under different degrees of surface roughness. At low concentration of electron attaching gas ($\sim$10%), the breakdown strengths of the mixtures can be optimized by maintaining the suitable amount of attaching gases in N_2. One very surprising result is that 2-C_4F_6, which possesses the highest dielectric strength among the other three gases, suffers the most loss from surface roughness. Figure 23 indicates that the ratio V_R/V_{SM} of 2-C_4F_6 drops below 0.7 at 40% concentration and at a groove depth of 0.02-inch. (The breakdown voltage measurements went to 40% only because of the limitation of the high voltage power supply which has a range from 0 to 150-KV and the breakdown voltages of 2-C_4F_6 at higher concentration exceed this limit). Although SF_6 has the lowest dielectric strength as compared with other fluorocarbons, its mixture with N_2 has the highest breakdown voltages at low concentration ($\lesssim$ 10%). This effect is shown in Figure 12

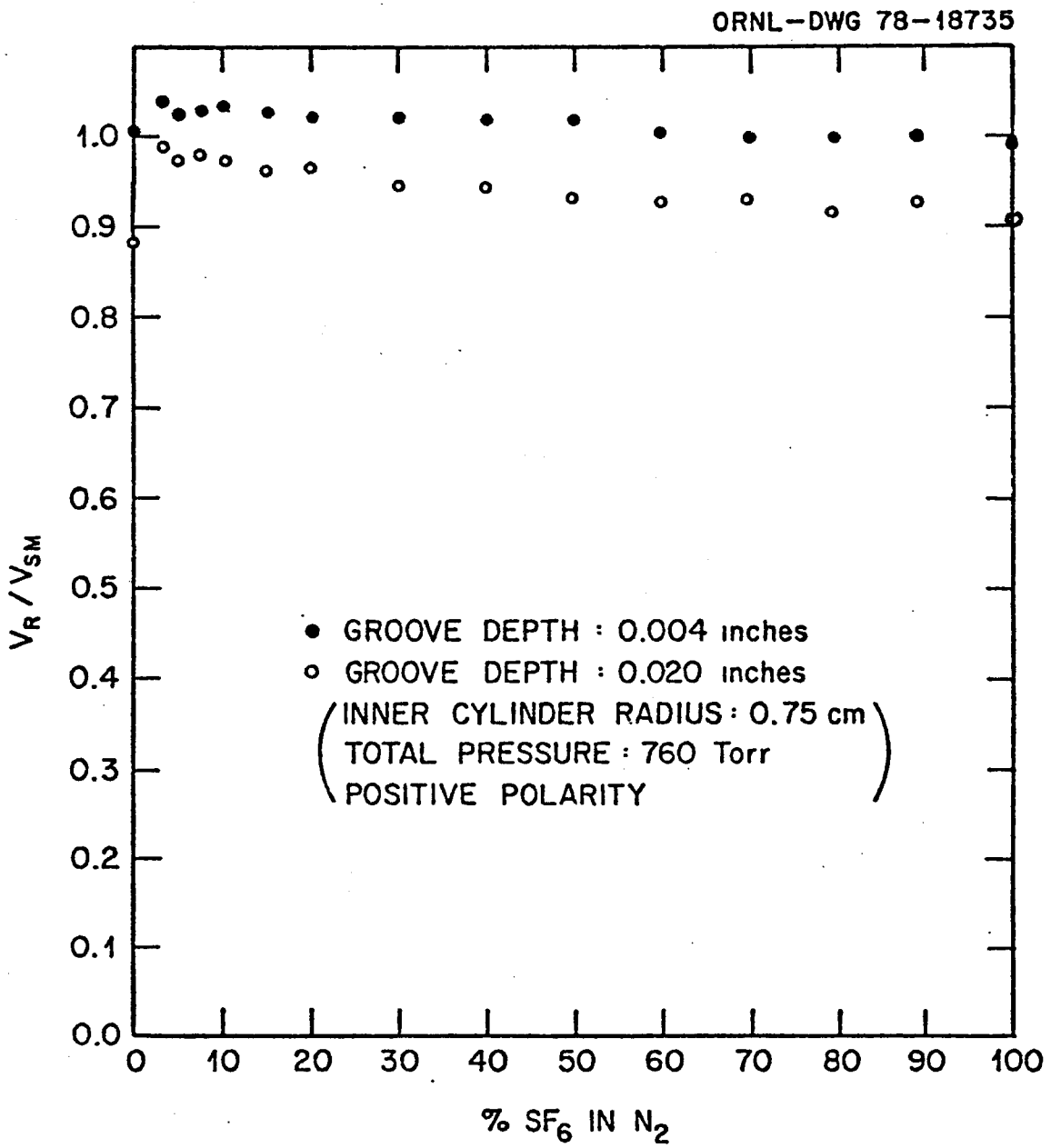


Figure 16. Ratios of breakdown voltages for SF_6/N_2 mixtures with rough (grooved) inner electrodes (V_R) and with smooth electrodes (V_{SM}) of 0.75-cm radius at positive potential.

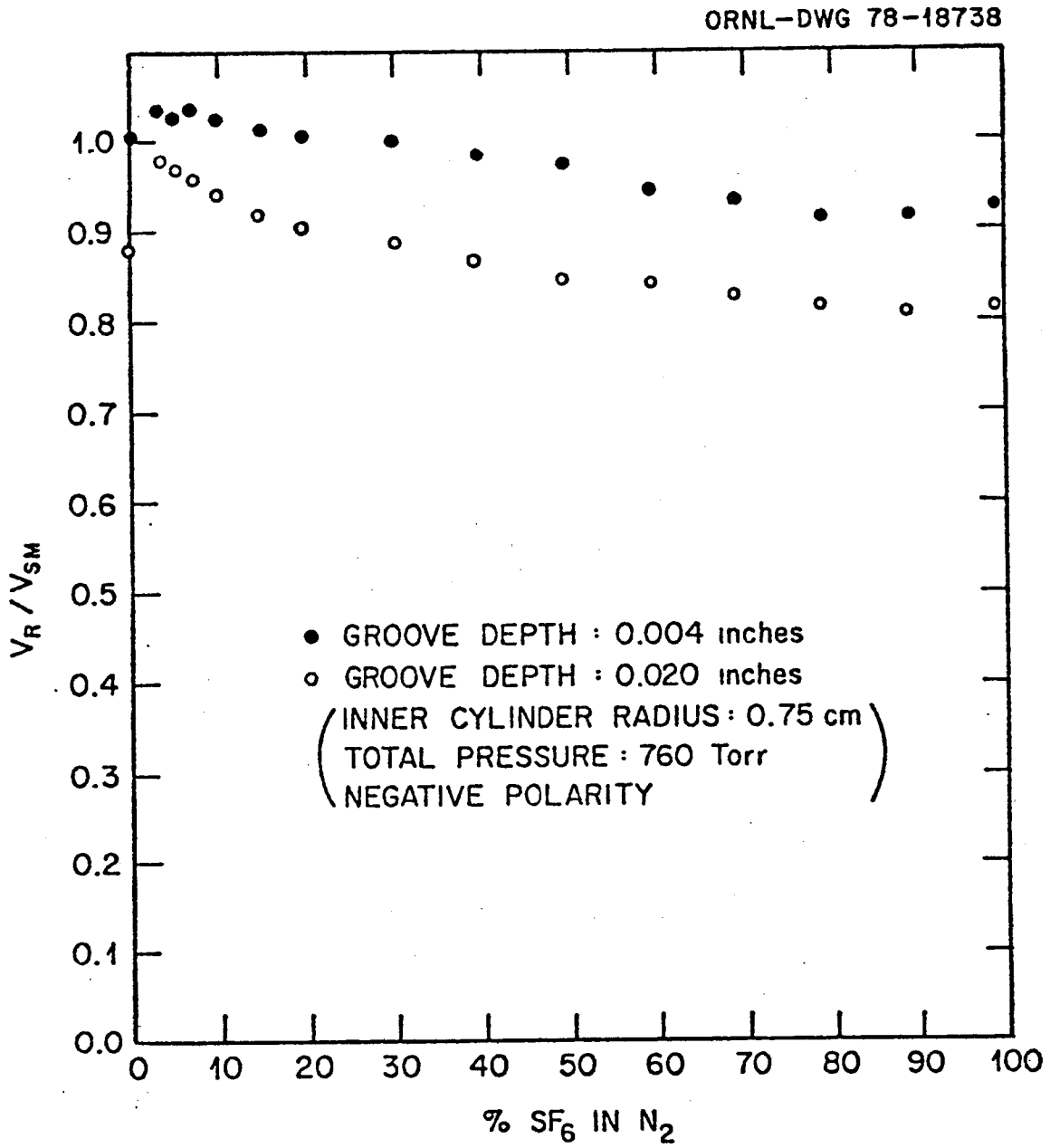


Figure 17. Ratios of breakdown voltages for SF_6/N_2 mixtures with rough (grooved) inner electrodes (V_R) and with smooth electrodes (V_{SM}) of 0.75-cm radius at negative potential.

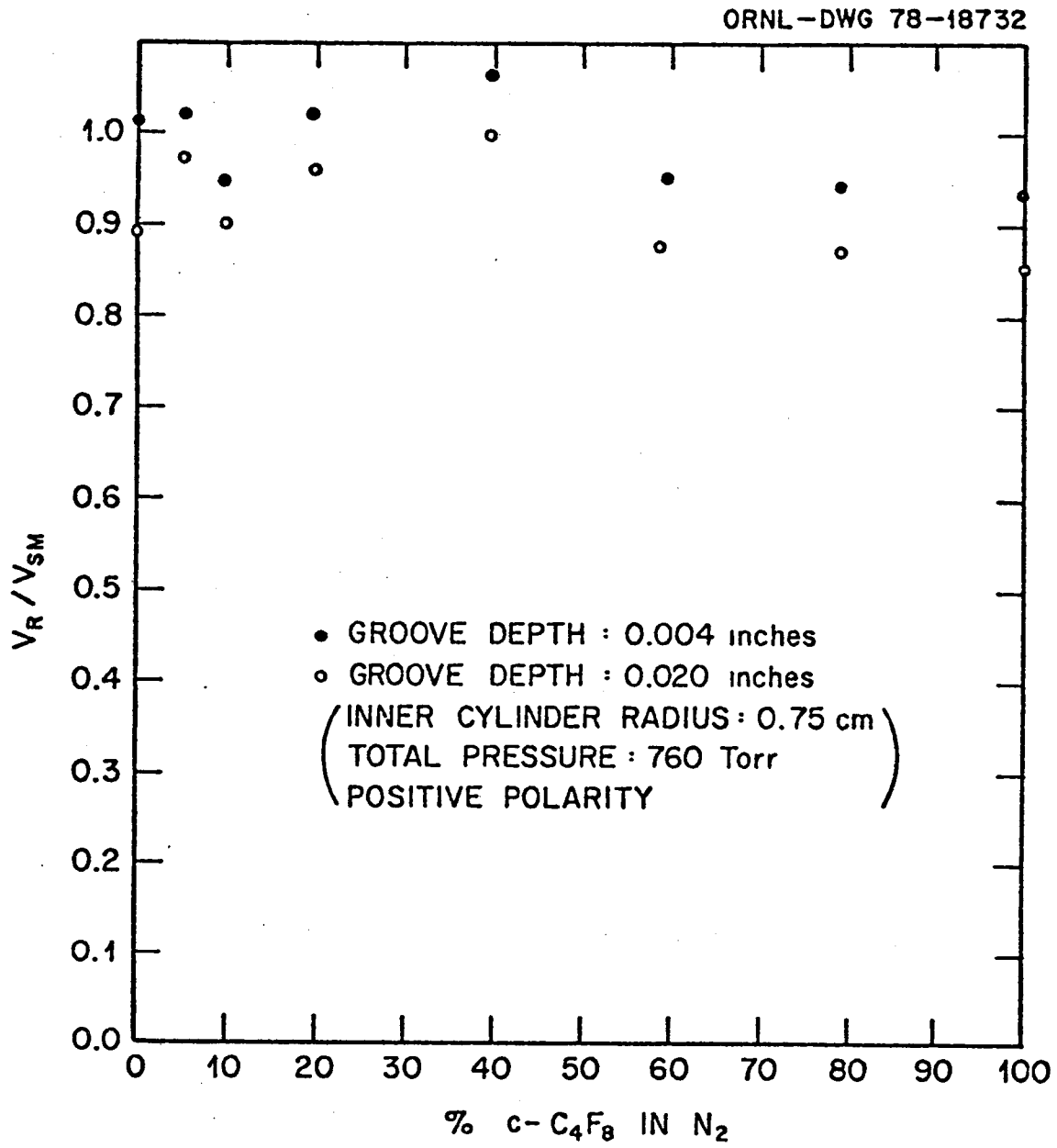


Figure 18. Ratios of breakdown voltages for c-C_4F_8/N_2 mixtures with rough (grooved) inner electrodes (V_R) and with smooth electrodes (V_{SM}) of 0.75-cm radius at positive potential.

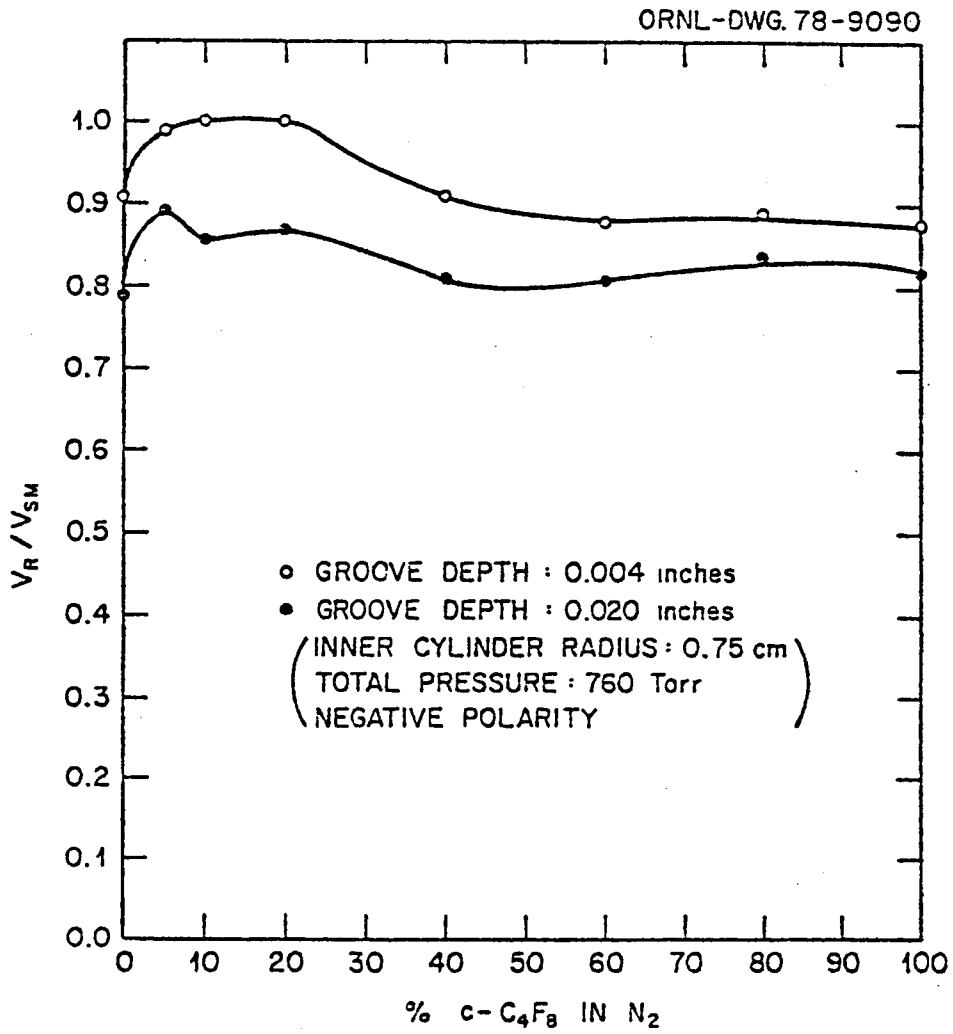


Figure 19. Ratios of breakdown voltages for c-C_4F_8/N_2 mixtures with rough (grooved) inner electrodes (V_R) and with smooth electrodes (V_{SM}) of 0.75-cm radius at negative potential.

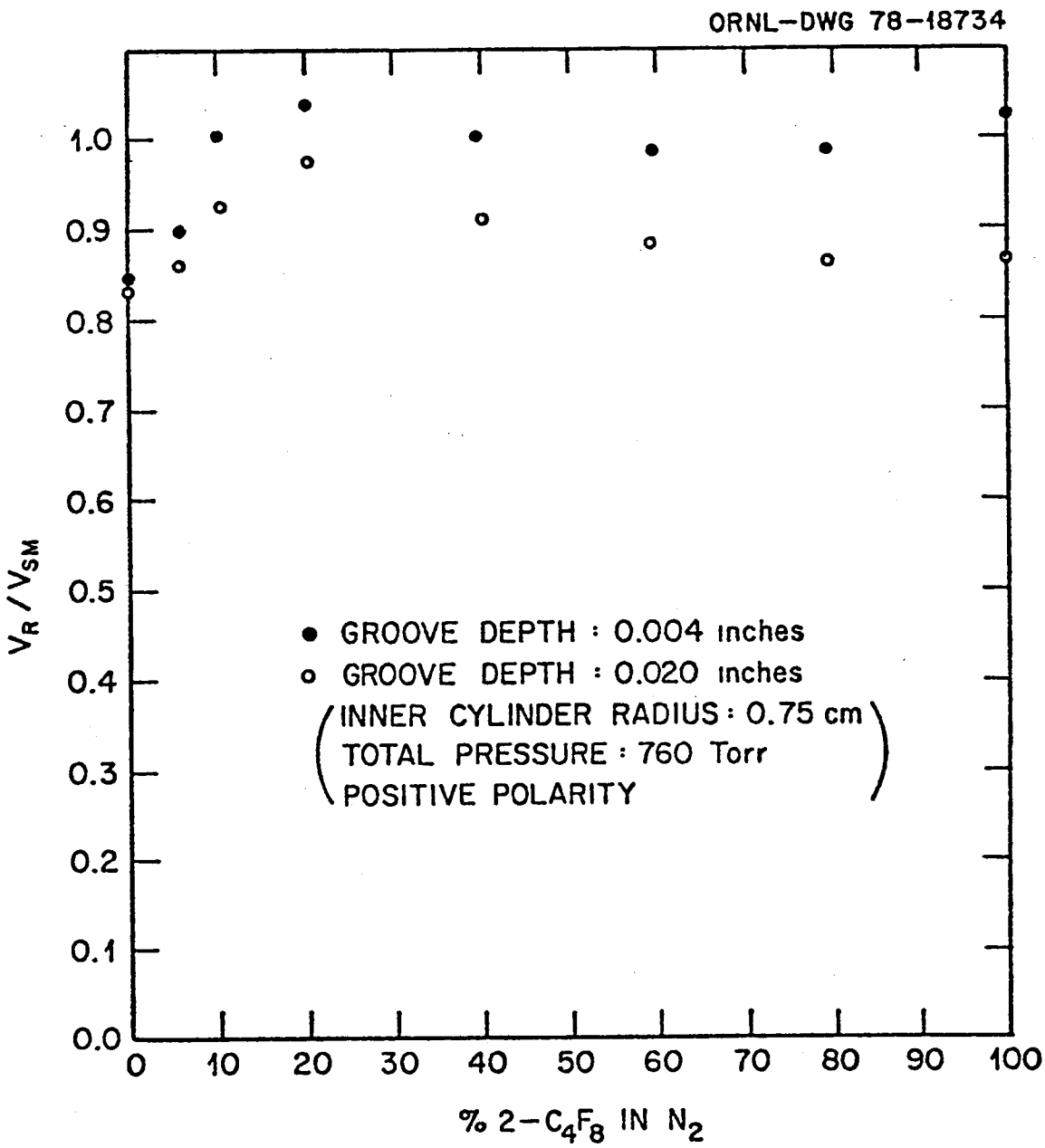


Figure 20. Ratios of breakdown voltages for 2-C_4F_8/N_2 mixtures with rough (grooved) inner electrodes (V_R) and with smooth electrodes (V_{SM}) of 0.75-cm radius at positive potential.

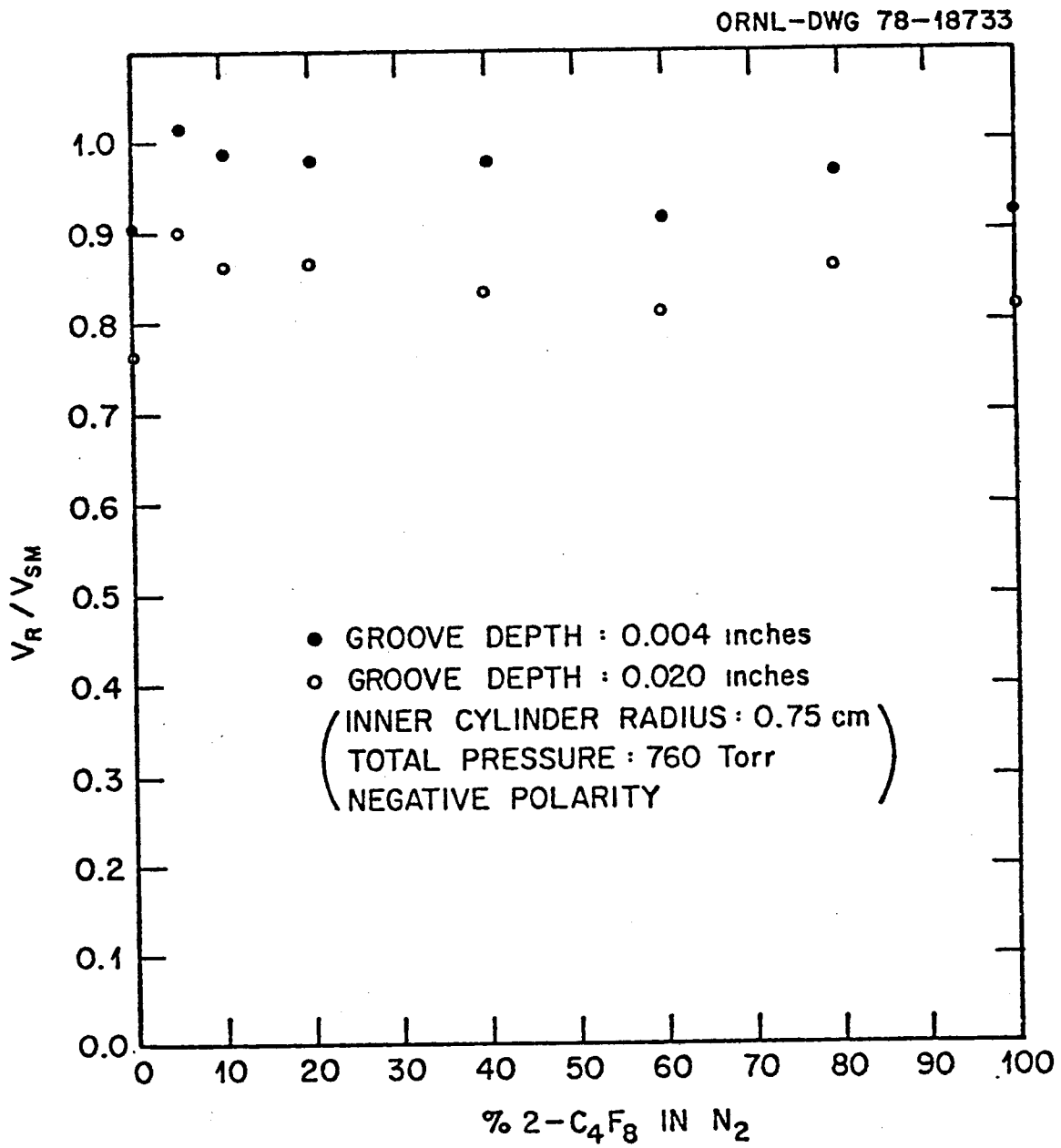


Figure 21. Ratios of breakdown voltages for 2-C_4F_8/N_2 mixtures with rough (grooved) inner electrodes (V_R) and with smooth electrodes (V_{SM}) of 0.75-cm radius at negative potential.

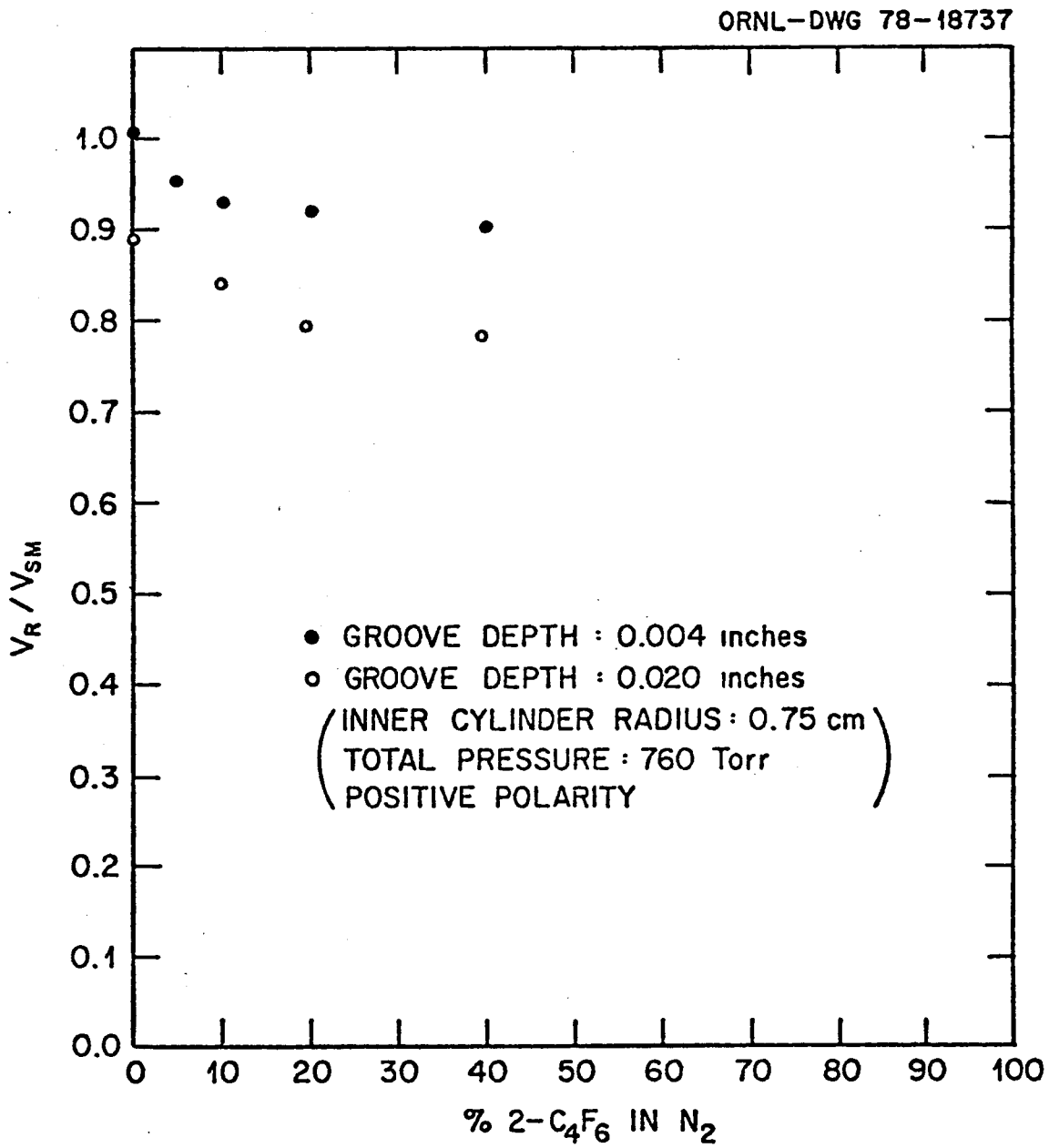


Figure 22. Ratios of breakdown voltages for 2-C_4F_6/N_2 mixtures with rough (grooved) inner electrodes (V_R) and with smooth electrodes (V_{SM}) of 0.75-cm radius at positive potential.

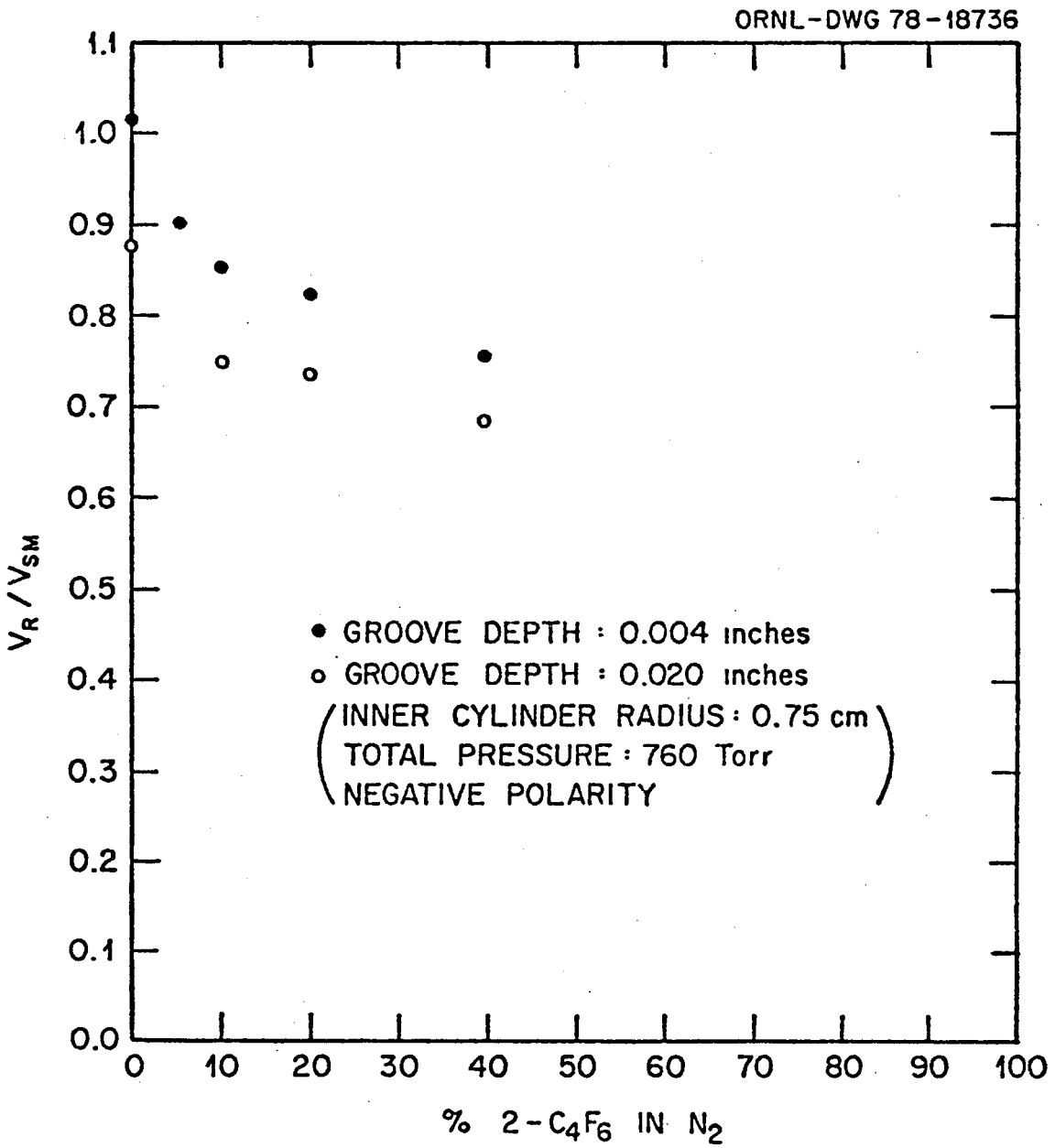


Figure 23. Ratios of breakdown voltages for 2-C_4F_6/N_2 mixtures with rough (grooved) inner electrodes (V_R) and with smooth electrodes (V_{SM}) of 0.75-cm radius at negative potential.

to Figure 15. Especially with higher degree of roughness, this superiority of SF_6 can be seen more clearly. For example, in Figure 15 the breakdown voltage of SF_6 is the highest even at 20%. This result proves that SF_6 has better abilities to handle surface roughness than the fluorocarbons at lower concentration in N_2.

The Effects of Electrode Materials

Three 1.4-cm radius electrodes of different materials have been made to study the effects of electrode materials on the dielectric strengths of gases. The materials are stainless steel, aluminum, and copper. The results are summarized in Table 1. This table shows the percent variation of breakdown voltages of other materials as compared with stainless steel. The positive signs indicate higher breakdown voltages, and the negative signs indicate lower breakdown voltages than with stainless steel. The absolute breakdown voltages of aluminum and copper can be found from the results already presented in Figures 8 to 11 and together with this table. Again the fluorocarbon/N_2 mixtures have higher breakdown voltages as compared to the corresponding SF_6/N_2 mixtures. However, the materials have no significant effects on the breakdown strengths of SF_6/N_2 mixtures. But the fluorocarbon/N_2 mixtures show higher percent variations of breakdown voltages with different materials. The average percent variation of each material is shown in Table 2 (sum of percent variation of each material ÷ number of percent variations). It can be

Table 1

% VARIATION OF BREAKDOWN VOLTAGES

FROM STAINLESS STEEL

	STAINLESS STEEL		ALUMINUM		COPPER	
% SF_6 in N_2	-ve	+ve	-ve	+ve	-ve	+ve
0	0	0	-7.3	-6.6	-9.4	-5.9
5	0	0	-7.1	-6.2	-7.4	-6.2
10	0	0	-4.9	-5.3	-5.2	-5.2
20	0	0	-5.9	-4.0	-5.4	-4.1
40	0	0	-4.3	-3.6	-3.9	-3.5
60	0	0	-4.2	-3.1	-3.3	-2.8
80	0	0	-3.3	-3.0	-2.9	-2.8
100	0	0	-4.3	-1.9	-3.1	-2.1
% c-C_4F_8 in N_2						
0	0	0	-7.3	-6.6	-9.4	-5.9
5	0	0	4.8	7.3	8.2	7.9
10	0	0	7.2	8.4	10.2	10.0
20	0	0	4.7	7.4	9.3	9.7
40	0	0	1.3	4.3	6.4	8.4
60	0	0	12.0	7.5	18.5	14.1
80	0	0	8.1	9.0	15.9	16.2
100	0	0	-0.6	6.1	9.1	12.9
% 2-C_4F_8 in N_2						
0	0	0	-7.3	-6.6	-9.4	-5.9
5	0	0	0.6	3.2	2.5	2.6
10	0	0	4.6	6.3	6.0	5.9
20	0	0	7.0	8.5	6.5	4.9
40	0	0	14.3	22.9	11.7	19.1
60	0	0	18.2	16.6	14.1	10.9
80	0	0	16.4	10.8	9.1	3.1
100	0	0	12.5	7.4	3.7	-1.8
%2-C_4F_6 in N_2						
0	0	0	-7.3	-6.6	-9.4	-5.9
5	0	0	-8.3	-7.4	-9.1	-6.0
10	0	0	-6.6	-3.1	-3.4	-1.6
20	0	0	-9.6	-9.0	-4.9	-2.4
40	0	0	-11.0	-2.2	-9.2	-0.2

Table 2

AVERAGE % VARIATION OF BREAKDOWN VOLTAGES

FROM STAINLESS STEEL

	ELECTRODE MATERIALS	-VE INNER ELECTRODE	+VE INNER ELECTRODE
SF_6/N_2	Stainless steel	0	0
	Aluminum	-5.2	-4.2
	Copper	-5.1	-4.1
$c\text{-}C_4F_8/N_2$	Stainless Steel	0	0
	Aluminum	3.8	5.4
	Copper	8.5	9.2
$2\text{-}C_4F_8/N_2$	Stainless Steel	0	0
	Aluminum	8.3	8.7
	Copper	5.5	4.9
$2\text{-}C_4F_6/N_2$	Stainless Steel	0	0
	Aluminum	8.6	5.7
	Copper	7.2	3.2

seen from Table 2 that the average percent variations of SF_6/N_2 mixtures is about 5% while the average percent variations of fluorocarbon/N_2 mixtures can swing up to about 9%. These variations could be due to the effects of coating of oxide films on the electrodes after spark breakdowns. The exact cause of these deviations has yet to be found.

The Effects of Particle Contaminants

It has been realized that conducting particles can seriously reduce the dielectric strength of gaseous insulating system (20,21). Therefore, it is worthwhile to investigate the effects and behavior of conducting particles in practical systems. To study these effects, five copper wire particles of dimensions 1/8-inch long by 0.015-inch diameter are introduced into the central inter-electrode region. Two Lexan disc barriers with a central hole of 0.75-cm radius are inserted into the open ends of the outer cylinder electrode to block the particles from escaping the central inter-electrode region. The breakdown results of each mixture can be compared to the results of the corresponding mixture without particles. The breakdown strengths of all insulating mixtures have been found reduced by a factor of approximately 3. Figures 24 and 25 present the breakdown voltages for the mixtures in the presence of particles (17).

The breakdown curves of SF_6/N_2 mixtures with these particles still show their characteristic saturation effects while the fluorocarbon/N_2 mixtures are always in a straight line except that their breakdown voltages are very much lowered.

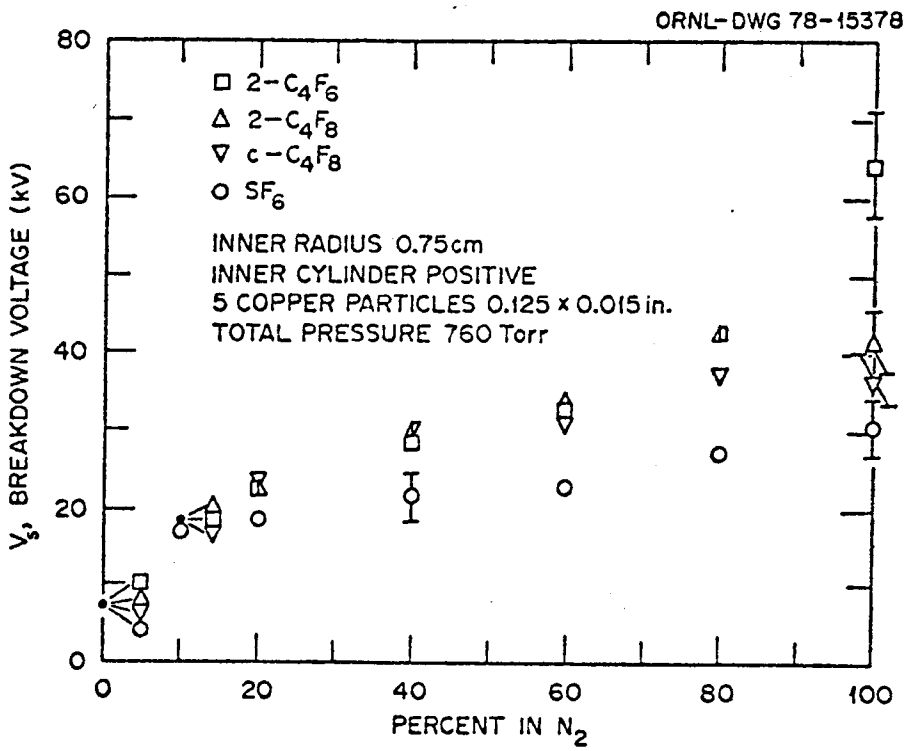


Figure 24. Breakdown voltages of SF_6/N_2 mixtures and fluorocarbon/N_2 mixtures in the presence of copper wire particles with 0.75-cm radius inner electrodes at positive potential.

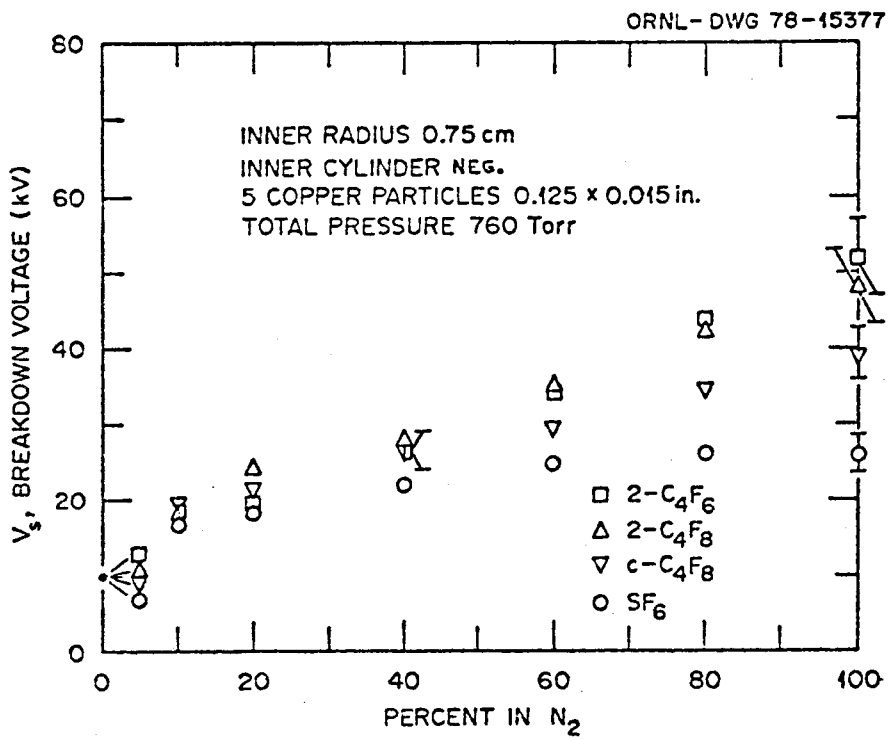


Figure 25. Breakdown voltages of SF_6/N_2 mixtures and fluorocarbon/N_2 mixtures in the presence of copper wire particles with 0.75-cm radius inner electrodes at negative potential.

Direct observations of particle behavior between the concentric cylinders indicate that the particles adopt two major characteristic motions. As the voltage increases to a characteristic value independent of the gas, the particles are suddenly elevated by the electric field and start bouncing between the electrodes. As the voltage increases further, and if no breakdown occurs first, the particles hover perpendicularly at the negative electrode with visible light emitting from the ends close to the negative electrode and this is known as the "firefly" motion. It is observed that each breakdown is caused by a single free particle. The particles are lifted at approximately a constant voltage and stop moving at a voltage much lower than the liftoff voltage independent of the gas mixture. The liftoff voltage is at 17.0 $\pm$1.5-KV and the stopping voltage is at 7.0 $\pm$1.5-KV.

CHAPTER IV

CONCLUSION

The fundamental knowledge of electron-molecule interactions has been applied to the design of good gaseous dielectrics. In this research four types of binary gaseous dielectric mixtures (SF_6/N_2, c-C_4F_8/N_2, 2-C_4F_8/N_2, and 2-C_4F_6/N_2) of various proportions with conditions corresponding to practical systems have been studied. These binary gaseous mixtures are chosen so that they consist basically of one electron-attaching gas and one electron-thermalizing gas. The dielectric gases attach electrons only at some low energy range. SF_6, which is the weakest dielectric, attaches electrons up to $\sim$0.4eV while the strongest dielectric, 2-C_4F_6, attaches electrons up to $\sim$1.4eV (see Figures 1 and 2 on pages 13 and 15). Electrons with energy exceeding this energy range will accelerate under the electric field and gain more and more energy for ionization of the neutral gas molecules, resulting in a Townsend or streamer type breakdown. Therefore, a thermalizing gas is added to the dielectric gas for slowing down these electrons and returning them to the attachment energy range for effective capture. In this research nitrogen, which has negative ion resonances (see Figure 2 on page 15) from about 2 to 3eV, was used as the electron thermalizing gas.

The dielectric strengths of these binary mixtures have been tested in three different sets of concentric cylinders. All these tests were performed at a total gas pressure of one

atmosphere and at room temperature ($\sim 21^{\circ}C$). It was concluded in Chapter II that a good dielectric should have a large attachment cross section extending over a wide electron attachment energy range. SF_6, which has the narrowest attachment energy range ($\sim 0.4eV$), has turned out to be the weakest dielectric just as predicted. SF_6/N_2 mixtures have lower breakdown voltages than the other three fluorocarbon/N_2 mixtures and exhibit a saturation effect. The breakdown curves of the fluorocarbon/N_2 mixtures are always in a straight line with breakdown strengths in the decreasing order 2-C_4F_6/N_2, 2-C_4F_8/N_2, and c-C_4F_8. The relative breakdown strengths of fluorocarbon/N_2 mixtures with respect to SF_6/N_2 mixtures in different cylindrical geometries are given in Table 3.

The effects of surface roughness have been studied with inner electrodes with spiralling grooves. The breakdown strengths of the fluorocarbon/N_2 mixtures are still better than the SF_6/N_2 mixtures except at very low proportions of fluorocarbons with N_2. At about or below 10% attaching gas, SF_6/N_2 mixtures have higher breakdown voltages with roughness. Also, results indicate that all four binary mixtures are least sensitive to surface roughness at approximately 5% attaching gas plus 95% nitrogen. Thus, the dielectric strengths of the mixtures can be optimized by controlling the appropriate proportions of attaching gases in nitrogen.

Three inner electrodes made of different materials have been used to study the effects of electrode materials on dielectric strengths of gases. The materials are stainless

Table 3

RELATIVE DIELECTRIC STRENGTHS OF FLUOROCARBON/N_2 MIXTURES WITH RESPECT TO SF_6/N_2 MIXTURES

Component (%)	SF_6		$c\text{-}C_4F_8$		$2\text{-}C_4F_8$		$2\text{-}C_4F_6$	
	-ve	+ve	-ve	+ve	-ve	+ve	-ve	+ve
0.4-cm Electrode								
0	1.0	1.0	1.0	1.0	1.0	1.0	1.0	1.0
5	1.0	1.0	1.0	1.0	1.1	1.1	1.2	1.1
10	1.0	1.0	1.0	0.9	1.0	1.0	1.2	1.2
20	1.0	1.0	0.9	0.9	1.0	1.0	1.3	1.4
40	1.0	1.0	1.1	1.0	1.2	1.1	1.6	1.6
60	1.0	1.0	1.2	1.2	1.4	1.4	-	-
80	1.0	1.0	1.3	1.3	1.5	1.5	-	-
100	1.0	1.0	1.4	1.4	1.7	1.7	-	-
0.75-cm Electrode								
0	1.0	1.0	1.0	1.0	1.0	1.0	1.0	1.0
5	1.0	1.0	0.9	0.9	1.0	1.1	1.1	1.1
10	1.0	1.0	0.9	1.0	1.0	1.0	1.1	1.2
20	1.0	1.0	0.9	1.0	1.0	1.1	1.3	1.3
40	1.0	1.0	1.0	1.0	1.1	1.3	1.5	1.5
60	1.0	1.0	1.1	1.2	1.3	1.4	-	-
80	1.0	1.0	1.2	1.3	1.4	1.6	-	-
100	1.0	1.0	1.3	1.4	1.6	1.7	-	-
1.4-cm Electrode								
0	1.0	1.0	1.0	1.0	1.0	1.0	1.0	1.0
5	1.0	1.0	0.8	0.8	0.8	0.8	1.0	1.1
10	1.0	1.0	0.8	0.8	0.8	0.8	1.1	1.1
20	1.0	1.0	0.8	0.8	0.8	0.9	1.2	1.3
40	1.0	1.0	0.9	1.0	1.0	1.0	1.5	1.5
60	1.0	1.0	1.0	1.0	1.1	1.2	-	-
80	1.0	1.0	1.1	1.1	1.3	1.4	-	-
100	1.0	1.0	1.2	1.2	1.4	1.6	-	-

steel, aluminum, and copper. No significant material effects have been found in SF_6/N_2 mixtures. The breakdown voltages of each material are very close with only a few percent variation from stainless steel, and these deviations are within experimental errors. But the breakdown voltages of fluorocarbon/N_2 mixtures have a larger random scatter up to about 9%.

Copper particles have been introduced into the systems to study their behavior and effects on the dielectric strengths of gases. The presence of particles reduces the dielectric strength of each binary mixture by a factor of approximately 3. Again the fluorocarbon/N_2 mixtures are superior to SF_6/N_2 mixtures. The particles are lifted off and start bouncing between the electrodes at a constant voltage independent of the gas. They change to "firefly" motion at higher voltages. Once they are lifted off, they stop bouncing at a lower constant voltage independent of the gas.

The most efficient way to inhibit breakdown is to reduce the number of free electrons and the energy of the electrons remaining free in the gas. Thus, a combination of an electron-attaching gas and an electron slowing-down gas is most likely the optimum gaseous dielectric. However, the attaching gas and thermalizing gas must be chosen so that their cross sections should cover different but closely adjacent energy ranges. The impact ionization cross section has a relatively less important role than the attachment cross section. Therefore, only the attchment cross sections are used in designing good dielectrics. This research has investigated four such binary

mixtures in practical systems with impressive results. In practical engineering applications, the pressure and temperature effects are also very important, but they are beyond the scope of this thesis. Further study is needed to develop engineering design rules and application to power apparatus.

LIST OF REFERENCES

LIST OF REFERENCES

1. L. G. Christophorou. "Elementary Electron-Molecule Interaction and Negative Ion Resonances at Subexcitation Energies and Their Significance in Gaseous Dielectrics". Proceedings of the XIII International Conference on phenomena in ionized gases, Berlin. September 11-17, 1977, vol. II, (1978).

2. M. O. Pace, L. G. Christophorou, D. R. James, R. Y. Pai, R. A. Mathis, and D. W. Bouldin. "Improved Unitary and Multicomponent Gaseous Insulators". IEEE Transactions on Electrical Insulation, vol. EI-13, Feb. 1978, pp. 31-36.

3. J. M. Meek and J. D. Craggs. Electric Breakdown of Gases. Oxford: Clarendon Press, 1953.

4. J. D. Cobine. Gaseous Conductors. New York: Dover, 1958.

5. L. B. Loeb and J. M. Meek. The Mechanism of the Electric Spark. California: Stanford University Press, 1941.

6. I. Alexeff. "Spark Breakdown-An Electrostatic Criterion". IEEE Transactions Plasma Science Conference. Tennessee: University of Tennessee, April 10-12, 1972.

7. H. Raether. Electron Avalanches and Breakdown in Gases. London: Butterworth's, 1964.

8. A. Pedersen. "Criteria for Spark Breakdown in Sulphur Hexafluoride". IEEE Trans. Power Apparatus and Systems, vol. PAS-89, No. 8, Nov/Dec. 1970.

9. J. M. Meek. Phys. Rev. 57(1940), 722.

10. M. S. Bhalla and J. D. Craggs. "Measurement of Ionization and Attachment Coefficients in Sulphur Hexafluoride in Uniform field". Proc. Phys. Soc., vol. 80, London, 1962, pp. 151-160.

11. R. W. Crowe and J. C. Devins. "On the Electric Breakdown of Electronegative Gases". Ann. Rep. NRC. Conf. Electrical Insulation. Washington: National Research Council, Publication 396, 1956, pp. 1-4.

12. L. G. Christophorou, D. R. James, R. Y. Pai, M. O. Pace, R. A. Mathis, and D. W. Bouldin. "Breakdown Strengths of Gaseous and Liquid Insulators", High Voltage Research. Report ORNL/TM-5604, Sept. 1976.

13. L. G. Christophorou, D. R. James, R. Y. Pai, M. O. Pace, R. A. Mathis, and D. W. Bouldin. "Breakdown Strengths of Gaseous and Liquid Insulators", High Voltage Research. Report ORNL/TM-5917, March 1977.

14. L. G. Christophorou. Atomic and Molecular Radiation Physics. New York: Wiley-Interscience, 1971.

15. D. R. James, L. G. Christophorou, R. Y. Pai, M. O. Pace, R. A. Mathis, I. Sauers, and C. C. Chan. "Dielectric Strengths of New Gases and Gas Mixture". Proceedings of the International Symposium on Gases Dielectrics, Knox., Tenne., Mar. 6-8, 1978, CONF-780301.

16. L. G. Christophorou, D. R. James, R. Y. Pai, M. O. Pace, R. A. Mathis, D. W. Bouldin, and D. E. Tittle. "Breakdown Strengths of Gaseous and Liquid Insulators" High Voltage Research. Report ORNL/TM-5806, Feb. 1977.

17. M. O. Pace, C. C. Chan, and L. G. Christophorou. "Application of Basis Gas Research to Practical Systems". 7th IEEE/PES Conference and Exposition on Overhead and Underground Transmission and Distribution, April 1979 (to be published).

18. L. G. Christophorou, D. R. James, R. Y. Pai, M. O. Pace, R. A. Mathis, D. W. Bouldin, A. A. Christodulides, and C. C. Chan. "Breakdown Strengths of Gaseous and Liquid Insulators", High Voltage Research. Report ORNL/TM-6113, Nov. 1977.

19. L. G. Christophorou, D. R. James, R. Y. Pai, R. A. Mathis, I. Sauers, M. O. Pace, D. W. Bouldin, A. A. Christodoulides, and C. C. Chan. "Breakdown Strengths of Gaseous and Liquid Insulators", High Voltage Research. Report ORNL/TM-6384, June 1978.

20. C. M. Cooke, R. E. Wooton, A. H. Cookson, "Influence of Particle on AC and DC Electrical Performance of Gas Insulated Systems at Extra-high Voltage". IEEE Trans., vol. PAS-96, 1977, pp. 558-564.

21. A. H. Cookson, P. C. Bolin, H. C. Doepken, Jr., R. E. Wooton, C. M. Cooke, and J. G. Trump. "Recent Research in the United States on the Effect of Particle Contamination Reducing the Breakdown Voltage in Compressed Gas-Insulated Systems". CIGRE paper for Paris meeting 1976.

APPENDIX

APPENDIX I

Below is a list of the costs and manufacturers of the dielectric gases used in this research:

1. Hexafluoro-2-butyne (2-C_4F_6), manufactured by Columbia Organic Chemicals Company, Inc. Columbia, S. C. The cost is \$600/Kg.
2. Perfluorobutene-2 (2-C_4F_8), manufactured by the same company as above; and the cost is \$300/Kg.
3. Perfluorocyclobutane (c-C_4F_8), also manufactured by the company same as above; and the cost is \$300/Kg.
4. Sulfur Hexafluoride (SF_6), manufactured by Allied Chemicals and Air Products; and the cost is \$310.42/Kg.

VITA

Ching Chuen Chan was born in Hong Kong on July 15, 1952. His elementary and high school education was completed in his home city. In the fall of 1973 he came over to the United States and attended the University of Tennessee, Knoxville. By the spring of 1977 he had received a Bachelor of Science degree in Electrical Engineering. During these four years, he had worked intermittently for 12 months at Florida Power and Light Company as a cooperative student. After he was graduated, he accepted a research assistantship at the University of Tennessee and continued working toward a Master's degree. At present he is working as a research assistant in the Atomic, Molecular, and High Voltage Physics Group at Oak Ridge National Laboratory.